When each product ion spectrum of the peptide ions in this LC/ESI MS/MS analysis was identified by the computer program Mascot, the sequence coverage of apoB100 was 38%. The ions, *m/z* 1177.9 (+3) at 64 min, 1289.0 (+3) at 91 min, and 1053.2 (+3) at 84 min, were identified as TIHDLHLFIENIDFN[2212]KSGSSTASWIQNVDTK containing the potential *N*-glycosylation site Asn2212 (G7), SSVITLNTNAELFN[3331]QSDIVAHLLSSSSSVIDALQYK containing Asn3331 (G14), and DFHSEYIVSASN[4404]-FTSQLSSQVEQFLHR containing Asn4404 (G19), respectively (data not shown). These results indicate that some parts of these glycosylation sites were not glycosylated. There were many unexplained peptides and glycopeptides in the digest (data not shown). This may be due to the unexpected digestion or nonspecific cleavage of apolipoprotein B100 as well as the multiple isoforms of the proteins.

LC/ESI MS/MS analysis of chymotryptic digest of apoB100

To determine the carbohydrate at undetected glycosylation sites in the tryptic digest including Asn1341 and 1350 (G4 and G5), which belong to the same tryptic peptide, the chymotrypsin digest was analyzed by LC/ESI MS/MS using the same methodology. Figure 5A shows a TIC of the TOF MS scan for the full scan *m/z* 700–2000. The collision energy was adjusted at 40–80 eV depending on the precursor ions. A TIC of the product ion scan and extracted ion chromatogram at *m/z* 204.05–204.15 (HexNAc) are presented in Figure 5B and 5C, respectively.

Figure 6A shows the product ion spectrum of 768.4 (+2) at 14 min for the chymotryptic glycopeptide. The carbohydrate B^+ ions, y1 and b2 ions of peptide NW (residue 1341–1342), and peptide + GlcNAc ion were found in the product ion spectrum. The carbohydrate composition, $[HexNAc]_2[Hex]_5$, was deduced from the calculated carbohydrate molecular ion, 1234.6. Figure 6B shows the product ion spectrum of 1444.1 (+2) at 9 min for the glycopeptide. The carbohydrate B^+ ions, peptide and peptide + GlcNAc ions, and peptide fragment ions from the peptide SGGNTSTDHF (residue 1347–1356) were detected in the product ion spectrum. Carbohydrate molecular weight, 1882.8, was calculated and the oligosaccharide composition, $[HexNAc]_2[Hex]_6$, was deduced from the molecular weight. The peptide fragment ions were also detected in the product ion spectrum for the chymotryptic glycopeptides as tryptic glycopeptides. The peptide and peptide + GlcNAc ions were detected in product ion spectra. These ions helped us determine the peptide moiety of the glycopeptide ion.

Results of the site-specific analysis of glycosylation of the chymotryptic digest are summarized in Table III. The oligosaccharide heterogeneity at each of 13 *N*-glycosylation sites was determined by LC/ESI MS/MS from the chymotryptic digest of apoB100 (Table III).

Carbohydrate diversity of each site

Results for the tryptic digest and chymotryptic digest of apoB100 are listed in Table IV. The oligosaccharide composition and type were deduced based on the molecular weight and previously reported oligosaccharide structures of apoB100. No information on glycosylation at Asn7 and 2533 (G1 and 8) was obtained from the analysis of the tryptic or chymotryptic digest. When the tryptic digest of apoB100 was analyzed by LC/ESI MS/MS with the MS range *m/z* 400–2000, the sequence coverage of apoB100 was 41% and tryptic peptides containing Asn7, 2212, 2533, or 2955 (G1, 7, 8, or 10) were detected (data not shown). Together with the result of LC/ESI MS/MS with the MS range *m/z* 1000–2000, Asn7 and 2533 (G1 and 8) were not glycosylated or glycosylated only under detection sensitivity, and Asn2212, 2955, 3331, and 4404 (G7, 10, 14, and 19) were partially glycosylated. These findings indicate that 17 of 19 potential *N*-glycosylation sites in apoB100 were glycosylated.

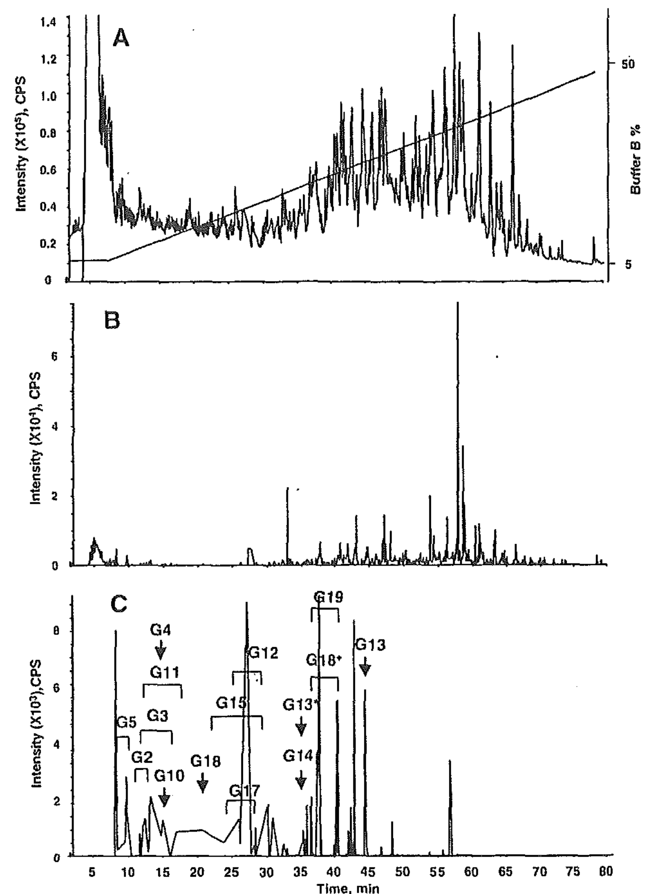

Fig. 5. LC/ESI MS/MS of chymotryptic digest of apolipoprotein B100. TIC of TOF MS scan for the full scan *m/z* 700–2000 and the HPLC gradient are indicated (**A**). TIC of the product ion scan data-dependently acquired (**B**). Extract ion chromatogram at *m/z* 204 of product ion spectra (**C**). Arrows and brackets denote glycopeptide fraction and *N*-glycosylation site ID. G13* was found to be oxidized at a methionine residue. G18⁺ was found as missed cleaved glycopeptides.

The most heterogeneous oligosaccharides were found at Asn3384 (G15). Asn3384 possessed neutral or monosialylated hybrid and monoantennary complex type and mono- or disialylated biantennary complex type oligosaccharides as well as one high-mannose type oligosaccharide. Asn158, 1341, 1350, 3309, and 3331 (G2, 4, 5, 13, and 14) were occupied by high-mannose type oligosaccharides, whereas Asn956, 1496, 2212, 2752, 2955, 3074, 3197, 3438, 3868,

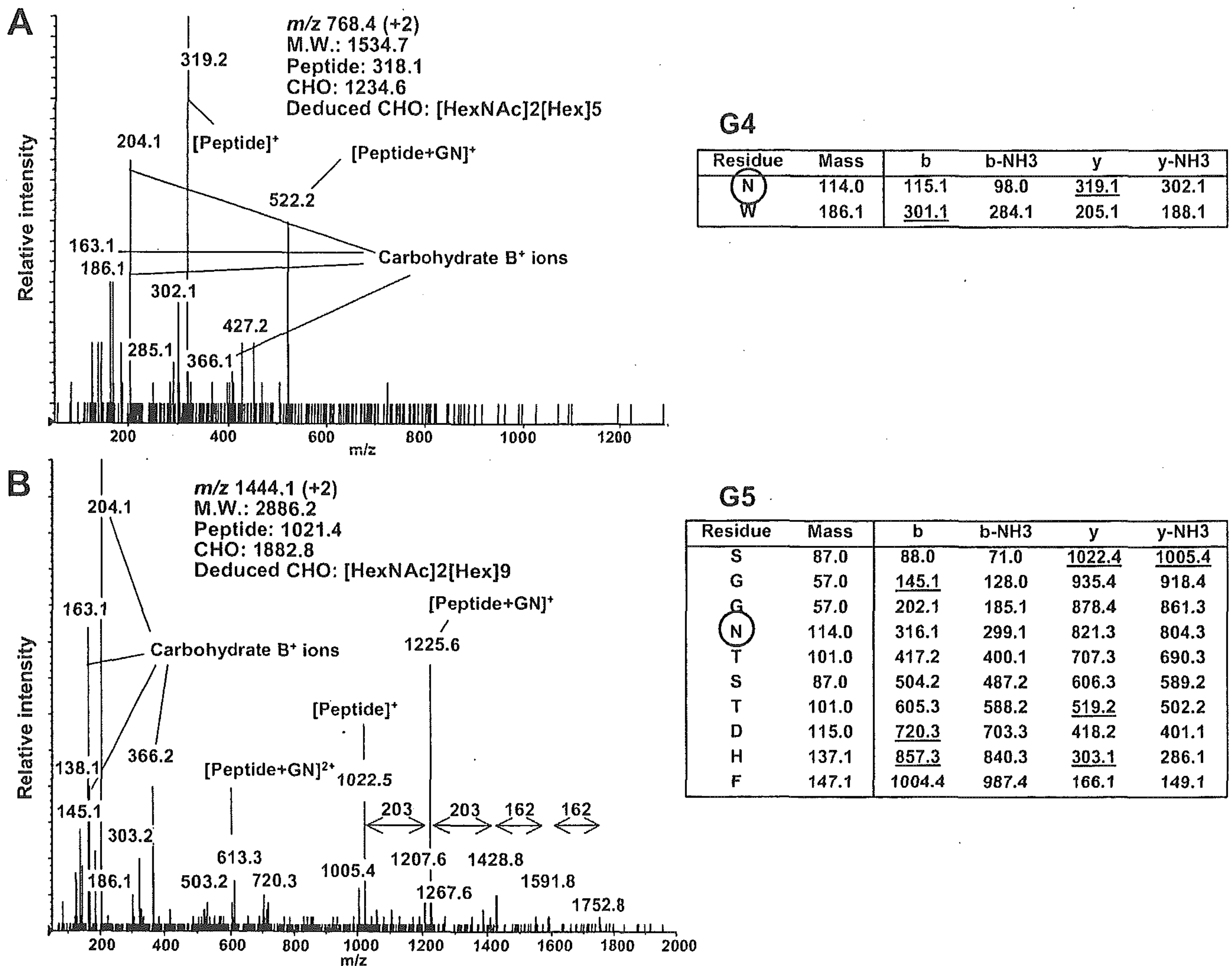

G4

Residue	Mass	b	b-NH3	y	y-NH3
(N)	114.0	115.1	98.0	319.1	302.1
W	186.1	301.1	284.1	205.1	188.1

G5

Residue	Mass	b	b-NH3	y	y-NH3
S	87.0	88.0	71.0	1022.4	1005.4
G	57.0	145.1	128.0	935.4	918.4
G	57.0	202.1	185.1	878.4	861.3
(N)	114.0	316.1	299.1	821.3	804.3
T	101.0	417.2	400.1	707.3	690.3
S	87.0	504.2	487.2	606.3	589.2
T	101.0	605.3	588.2	519.2	502.2
D	115.0	720.3	703.3	418.2	401.1
H	137.1	857.3	840.3	303.1	286.1
F	147.1	1004.4	987.4	166.1	149.1

Fig. 6. Product ion spectra of the chymotryptic *N*-glycosylated peptides of apoB100. (**A**) Product ion spectrum of *m/z* 768.4 (+2) at 14 min for the glycopeptide consisting of residues 1341–1342. Peptide b and y ions of the peptide NW were found. Table shows *m/z* of the proposed b- and y-series fragment ions, and the detected ions are underscored. (**B**) Product ion spectrum of *m/z* 1444.1 (+2) at 9 min for the glycopeptide consisting of residues 1347–1356. Several ions are consistent with the b- and y-series fragment ions derived from the peptide SGGNTSTDHF. Table shows *m/z* of the proposed b- and y-series fragment ions, and the detected ions are underscored.

4210, and 4404 (G3, 6, 7, 9–12, and16–19) were predominantly occupied by monosialylated or disialylated biantennary complex type oligosaccharides (Figure 7).

Discussion

Although the role of the carbohydrate structures in LDL and/or apoB100 has been examined in several studies (Attie *et al.*, 1979; Filipovic *et al.*, 1979; Fujioka *et al.*, 2000; Orekhov *et al.*, 1989; Shireman and Fisher, 1979), it is still unknown. It is necessary to elucidate the diversity of the oligosaccharides at each *N*-glycosylation site. This is the first report on the characterization of *N*-linked oligosaccharides in apoB100 at each glycosylation site. The protein was initially carboxymethylated and digested with an enzyme (trypsin or chymotrypsin), and then the complex mixtures of peptides and glycopeptides were subjected to LC/ESI MS/MS analysis. Product ion scan of each precursor ion was carried out in a data-dependent manner. The glycopeptide molecular ions were easily distinguished from peptide ions by the presence of carbohydrate-related oxonium ions, such as *m/z* 204 (HexNAc), 186 (HexNAc–H_2O), 168 (HexNAc–H_2O), 366 (HexHexNAc), and others in product ion spectra. Furthermore, product ion spectra provided information for the elucidation of the amino acid sequence of the glycopeptides.

The oligosaccharide structure could be deduced based on the calculated molecular weight of the oligosaccharide moiety. The glycopeptide precursor ion was assigned using three strageties. (1) By comparing the product ions of the glycopeptide with the expected fragment ions derived from

Table III. Site-specific glycosylation analysis of the chymotryptic digest of apoB100 using LC/ESI MS/MS

			Glycopeptides			Oligosaccharide				
Glycosylation site ID	Retention time (min)	Peptide theoretical MW[a]	*m/z*	Charge	Calculated MW[a]	Calculated MW[a]	Theoretical MW[a]	Relative peak intensity (%)[b]	Composition[c]	Deduced Type[c]
G1	—	560.3	—	—	—	—	—	—	—	—
G2	11	822.3	1344.5	+2	2687.0	1882.7	1882.6	4	[HexNAc]2[Hex]9	High mannose
	11	822.3	1263.5	+2	2525.0	1720.7	1720.6	7	[HexNAc]2[Hex]8	High mannose
	11	822.3	1182.5	+2	2363.0	1558.7	1558.5	15	[HexNAc]2[Hex]7	High mannose
	12	822.3	1101.4	+2	2200.8	1396.5	1396.5	12	[HexNAc]2[Hex]6	High mannose
	12	822.3	1020.4	+2	2038.8	1234.5	1234.4	100	[HexNAc]2[Hex]5	High mannose
G3	12	1088.4	1001.8	+3	3002.4	1932.0	1931.7	70	[HexNAc]4[Hex]5[Neu5Ac]1	Biantennary complex
	15	1088.4	1098.8	+3	3293.4	2223.0	2222.8	100	[HexNAc]4[Hex]5[Neu5Ac]2	Biantennary complex
G4	14	318.1	768.4	+2	1534.8	1234.7	1234.4	—	[HexNAc]2[Hex]5	High mannose
G5	9	1021.4	963.1	+3	2886.3	1882.9	1882.6	100	[HexNAc]2[Hex]9	High mannose
	9	1021.4	1444.1	+2	2886.2	1882.8				
	9	1021.4	1363.1	+2	2724.2	1720.8	1720.6	40	[HexNAc]2[Hex]8	High mannose
	9[d]	1021.4	1282.1	+2	2562.2	1558.8	1558.5	16	[HexNAc]2[Hex]7	High mannose
G6	—	469.2	—	—	—	—	—	—	—	-
G7	—	1023.5	—	—	—	—	—	—	—	-
G8	—	515.3	—	—	—	—	—	—	—	-
G9	—	2846.4	—	—	—	—	—	—	—	-
G10	15	279.1	829.0	+3	2484.1	2223.0	2222.8	—	[HexNAc]4[Hex]5[Neu5Ac]2	Biantennary complex
	15	279.1	1243.0	+2	2484.0	2222.9				
G11	13	521.2	812.7	+3	2435.1	1931.9	1931.7	100	[HexNAc]4[Hex]5[Neu5Ac]1	Biantennary complex
	13	521.2	1218.5	+2	2435.0	1931.8				
	16	521.2	909.8	+3	2726.3	2223.0	2222.8	52	[HexNAc]4[Hex]5[Neu5Ac]2	Biantennary complex
G12	28	878.5	1028.8	+3	3083.4	2222.9	2222.8	—	[HexNAc]4[Hex]5[Neu5Ac]2	Biantennary complex
G13	44	978.5	1341.6	+2	2681.2	1720.7	1720.6	31	[HexNAc]2[Hex]8	High mannose
	44	978.5	1260.6	+2	2519.1	1558.6	1558.5	50	[HexNAc]2[Hex]7	High mannose
	44	978.5	1179.5	+2	2357.1	1396.6	1396.5	100	[HexNAc]2[Hex]6	High mannose

Table III. continued

Glycosylation site ID	Retention time (min)	Peptide theoretical MW[a]	Glycopeptides *m/z*	Glycopeptides Charge	Glycopeptides Calculated MW[a]	Oligosaccharide Calculated MW[a]	Oligosaccharide Theoretical MW[a]	Relative peak intensity (%)[b]	Composition[c]	Deduced Type[c]
	44	978.5	1098.5	2	2195.0	1234.5	1234.4	75	[HexNAc]2[Hex]5	High mannose
	35[d]	995.5*	1349.6	+2	2697.1	1719.6	1720.6	16	[HexNAc]2[Hex]8	High mannose
	35[d]	995.5*	1268.5	+2	2535.0	1557.5	1558.5	49	[HexNAc]2[Hex]7	High mannose
	35	995.5*	1187.5	+2	2373.0	1395.5	1396.5	100	[HexNAc]2[Hex]6	High mannose
	35	995.5*	1106.5	+2	2211.0	1233.5	1234.4	89	[HexNAc]2[Hex]5	High mannose
G14	35	995.5	954.4	+3	2860.3	1882.8	1882.6	—	[HexNAc]2[Hex]9	High mannose
	35	995.5	1431.2	+2	2860.3	1882.8				
G15	24	1128.5	1173.5	+2	2345.0	1234.6	1234.4	3	[HexNAc]2[Hex]5	High mannose
	24[d]	1128.5	1275.0	+2	2548.0	1437.5	1437.5	9	[HexNAc]3[Hex]5	Hybrid
	27	1128.5	1015.1	+3	3042.4	1931.9	1931.7	100	[HexNAc]4[Hex]5[Neu5Ac]1	Biantennary complex
	27	1128.5	947.4	+3	2839.3	1728.8	1728.6	79	[HexNAc]3[Hex]5[Neu5Ac]1	Hybrid
	27	1128.5	893.4	+3	2677.3	1566.8	1566.6	23	[HexNAc]3[Hex]4[Neu5Ac]1	Monoantennary complex
	30	1128.5	1112.2	+3	3333.5	2223.0	2222.8	28	[HexNAc]4[Hex]5[Neu5Ac]2	Biantennary complex
G16	—	550.2	—	—	—	—	—	—	—	-
G17	28	490.2	899.4	+3	2695.2	2223.0	2222.8	—	[HexNAc]4[Hex]5[Neu5Ac]2	Biantennary complex
	28	490.2	1348.5	+2	2695.0	2222.8				
G18	21	1082.6	999.8	+3	2996.4	1931.8	1931.7	100	[HexNAc]4[Hex]5[Neu5Ac]1	Biantennary complex
	25	1082.6	1096.8	+3	3287.4	2222.8	2222.8	51	[HexNAc]4[Hex]5[Neu5Ac]2	Biantennary complex
	37	1229.6[†]	786.9	+4	3143.5	1931.9	1931.7	100	[HexNAc]4[Hex]5[Neu5Ac]1	Biantennary complex
	37	1229.6[†]	1048.8	+3	3143.5	1931.8				
	38	1229.6[†]	994.8	+3	2981.5	1769.9	1769.6	14	[HexNAc]4[Hex]4[Neu5Ac]1	Biantennary complex
	40	1229.6[†]	859.7	+4	3434.6	2223.0	2222.8	67	[HexNAc]4[Hex]5[Neu5Ac]2	Biantennary complex
	40	1229.6[†]	1145.9	+3	3434.6	2223.0				
G19	37	736.4	884.4	+3	2650.3	1931.9	1931.7	100	[HexNAc]4[Hex]5[Neu5Ac]1	Biantennary complex
	37	736.4	1326.1	+2	2650.2	1931.8				
	40	736.4	981.4	+3	2941.2	2222.8	2222.8	94	[HexNAc]4[Hex]5[Neu5Ac]2	Biantennary complex

[a]Monoisotopic mass value.
[b]Relative peak intensity was calculated by comparing same chage state glycopeptide ions. The intensity of glycoform with maximum intensity at each glycosylation site was considered as 100%.
[c]The oligosaccharide composition and type were deduced from its composition.
[d]Product ion spectra were not acquired. These ions were considered as glycopeptides by the mass differences of 162(Hex) or 203(HexNAc) from the glycopeptides.
*The glycopeptides including G13 were found to be oxidized at methionine residue.
[†]Peptides of these glycopeptides including G18 were found as missed cleaved. The peptide sequence was considered as SKVHN[4210]GSEILF.

Table IV. Summary of apoB100 oligosaccharide structure obtained from tryptic digest and chymotryptic digest

Glycosylation site ID	Deduced oligosaccharide composition[a]					Deduced oligosaccharide type[a]
G1	Not glycosylated					—
G2	[HexNAc]2[Hex]9	[HexNAc]2[Hex]8	[HexNAc]2[Hex]7	[HexNAc]2[Hex]6	[HexNAc]2[Hex]5	High mannose
G3	[HexNAc]4[Hex]5[Neu5Ac]1	[HexNAc]4[Hex]5[Neu5Ac]2				Biantenary complex
G4	[HexNAc]2[Hex]5					High mannose
G5	[HexNAc]2[Hex]9	[HexNAc]2[Hex]8	[HexNAc]2[Hex]7			High mannose
G6	[HexNAc]2[Hex]5					High mannose
	[HexNAc]3[Hex]7[Neu5Ac]1	[HexNAc]3[Hex]6[Neu5Ac]1	[HexNAc]3[Hex]5[Neu5Ac]1			Hybrid
	[HexNAc]3[Hex]4[Neu5Ac]1					Monoanntenary complex
	[HexNAc]4[Hex]4[Neu5Ac]1	[HexNAc]4[Hex]5[Neu5Ac]1	[HexNAc]4[Hex]5[Neu5Ac]2			Bianntenary complex
G7	[HexNAc]4[Hex]5[Neu5Ac]1	[HexNAc]4[Hex]5[Neu5Ac]2				Bianntenary complex
G8	Not glycosylated					—
G9	[HexNAc]4[Hex]5[Neu5Ac]2					Bianntenary complex
G10	[HexNAc]4[Hex]5[Neu5Ac]1	[HexNAc]4[Hex]5[Neu5Ac]2				Bianntenary complex
G11	[HexNAc]4[Hex]5[Neu5Ac]1	[HexNAc]4[Hex]5[Neu5Ac]2				Bianntenary complex
G12	[HexNAc]4[Hex]5[Neu5Ac]2					Bianntenary complex
G13	[HexNAc]2[Hex]8	[HexNAc]2[Hex]7	[HexNAc]2[Hex]6	[HexNAc]2[Hex]5		High mannose
G14	[HexNAc]2[Hex]9					High mannose
G15	[HexNAc]2[Hex]5					High mannose
	[HexNAc]3[Hex]6	[HexNAc]3[Hex]5	[HexNAc]3[Hex]6[Neu5Ac]1	[HexNAc]3[Hex]5[Neu5Ac]1		Hybrid
	[HexNAc]3[Hex]4[Neu5Ac]1					Monoanntenary complex
	[HexNAc]4[Hex]4	[HexNAc]4[Hex]5	[HexNAc]4[Hex]4[Neu5Ac]1	[HexNAc]4[Hex]5[Neu5Ac]1	[HexNAc]4[Hex]5[Neu5Ac]2	Bianntenary complex
	[HexNAc]4[Hex]5[Neu5Ac]1[Fuc]1					Bianntenary complex
G16	[HexNAc]3[Hex]4[Neu5Ac]1					Monoanntenary complex
	[HexNAc]4[Hex]4[Neu5Ac]1	[HexNAc]4[Hex]5[Neu5Ac]1	[HexNAc]4[Hex]5[Neu5Ac]2			Bianntenary complex
G17	[HexNAc]4[Hex]5[Neu5Ac]1	[HexNAc]4[Hex]5[Neu5Ac]2				Bianntenary complex
	[HexNAc]5[Hex]6[Neu5Ac]2					Trianntenary complex
G18	[HexNAc]4[Hex]4[Neu5Ac]1	[HexNAc]4[Hex]5[Neu5Ac]1	[HexNAc]4[Hex]5[Neu5Ac]2			Bianntenary complex
G19	[HexNAc]4[Hex]5[Neu5Ac]1	[HexNAc]4[Hex]5[Neu5Ac]2				Bianntenary complex

[a]The oligosaccharide structure was deduced from the molecular weight and previously reported oligosaccharide structures of apoB100.

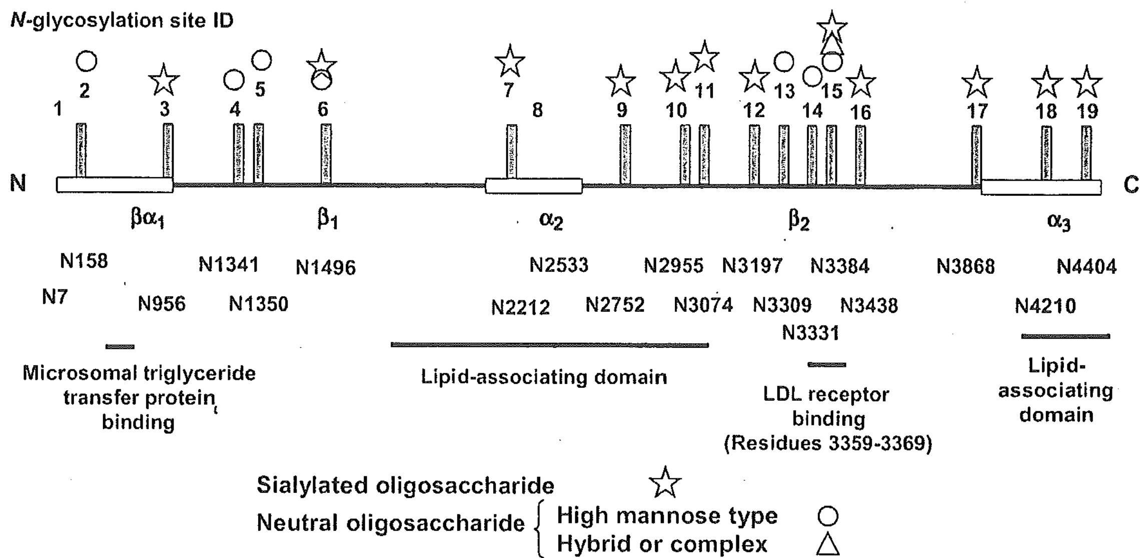

Fig. 7. *N*-glycosylation site of apoB100 and *N*-glycans at each site. *N*-glycosylation sites were shown on the pentapartite structure model, NH_3-$\beta\alpha_1$-β_1-α_2-β_2-α_3-COOH, previously reported (Segrest *et al.*, 1994). Circle, triangle, and star indicate high-mannose type oligosaccharides, neutral hybrid or neutral complex oligosaccharides, and mono- or disialylated oligosaccharides, respectively. High-mannose type oligosaccharides were found around the *N*-terminal and near the LDL–receptor binding site, and the other sites were attached by mono- or disialylated oligosaccharides. These oligosaccharide structures may reflect the local 3D structure of VLDL/LDL and may play a biological role.

the peptide containing the *N*-linked glycosylation site, we could directly deduce the peptide moiety. The molecular weight of the oligosaccharide moiety was calculated from the observed molecular weight of the glycopeptide and the theoretical molecular weight of the identified peptide. The carbohydrate composition and structure were deduced from the calculated molecular weight of the oligosaccharide. (2) There were relatively intense peaks of the peptide and peptide + GlcNAc ions in the glycopeptide product ion spectrum. Thus the *m/z* difference of 203 between fragment ions in the product ion spectrum could suggest the molecular weight of the peptide moiety. The peptide was determined from this suggested molecular weight and the molecular weight of the peptides containing the putative *N*-glycosylation site. The molecular weight of the carbohydrate was calculated, and the carbohydrate composition and structure were deduced. (3) Possible glycopeptide masses were calculated from the peptide masses containing the *N*-linked glycosylation site and possible *N*-linked oligosaccharide masses. The possible glycopeptide mass with the measured mass of the glycopeptide was identified. Assignment of peptide moiety was confirmed by the presence of the fragment ions derived from the peptide in the product ion spectrum.

The elution time as well as mass of a glycopeptide is also helpful to elucidate the oligosaccharide structure. The glycopeptides were eluted following reversed-phase high-performance LC based on the peptide and further separated based on the structure of the attached oligosaccharide (Kawasaki *et al.*, 2004). The glycopeptides having the same amino acid sequence were eluted in order of the number of Neu5Ac. Our results show that LC/ESI MS/MS with high sensitivity and high detection resolution is a powerful technique for the site-specific glycosylation analysis of glycoprotein.

Our study revealed that 17 of the 19 potential *N*-glycosylation sites in apoB100 were glycosylated, and the diversity of oligosaccharides at each of these *N*-glycosylation sites was determined. The deduced oligosaccharide structures in the present study were consistent with the structures previously identified in apoB100 (Garner *et al.*, 2001). Asn2212, which was reported to be unglycosylated (Yang *et al.*, 1989), could be glycosylated. The *N*-glycan structures and patterns are very different at each site. Asn158, 1341, 1350, 3309, and 3331 were occupied by high-mannose type oligosaccharides. The other sites except Asn1496 and 3384 (G6 and G15) were predominantly occupied by mono- or disialylated biantennary complex type oligosaccharides, and no neutral oligosaccharides were detected. These sialylated glycans may play an important biological role. Asn1496 and 3384 were occupied by high-mannose, hybrid, and complex type *N*-linked oligosaccharides. Hybrid-type oligosaccharides were found only at these two sites. The oligosaccharides at Asn 3384 are most heterogeneous, and at least 12 different oligosaccharide structures were present. Neutral complex type and neutral hybrid type oligosaccharides were detected only at this site. It is unlikely that this oligosaccharide heterogeneity is due to the fact that the apoB100 used in this study was extracted from the pooled serum of normolipidemic subjects, because no hybrid type oligosaccharides were detected except at Asn1496 and 3384 in this study, and it was reported that the diversity of the oligosaccharides of apoB100 was highly conserved among subjects (Garner *et al.*, 2001; Taniguchi *et al.*, 1989). It may be suggested that the diversity of the oligosaccharides at each glycosylation site was also conserved among subjects.

The relationship between sialylation and LDL–receptor binding has been examined. Desialylation of LDL increased the internalization of LDL by aortic smooth muscle cells

(Filipovic *et al.*, 1979), macrophage (Fujioka *et al.*, 2000) and aortic intimal cells (Orekhov *et al.*, 1989), but had no effect on degradation in hepatocytes (Attie *et al.*, 1979). These findings appear controversial. Asn3309, 3331, and 3384 are located near the LDL–receptor binding site in apoB100 (residues 3359–3369). Our data showed that these glycosylation sites were populated by high-mannose type (at Asn3309 and 3331) or a variety of oligosaccharides, including neutral or sialylated oligosaccharides (at Asn3384). These findings may indicate that sialic acid residues of apoB100 did not play a significant role in LDL–receptor binding and that desialylated LDL might be internalized by another mechanism. Shireman and Fisher (1979) reported that the removal of carbohydrate from LDL did not alter its binding to fibroblasts. Thus the carbohydrate moieties of LDL might not have a significant role in LDL–receptor binding.

The most interesting observation was that the most heterogeneous oligosaccharides were found at the *N*-glycosylation site (Asn3384) nearest to the LDL–receptor binding site. ApoB100 enwraps the VLDL and LDL particle. The C-terminal crosses over near the LDL–receptor binding site and inhibits binding of VLDL to the LDL receptor (Boren *et al.*, 1998). Conversion of VLDL to smaller LDL allows interaction with the LDL receptor. It is likely that the size of the VLDL/LDL particle could affect the 3D conformation around here. Thus the variety of oligosaccharide at Asn3384 may reflect the local 3D conformation of the VLDL particle and accessibility of trimming and glycosyl transferase enzymes.

The procedure described in this article provides an easy and efficient method for the identification of glycosylation sites and oligosaccharide heterogeneity of glycoproteins. Site-specific glycosylation analysis of apoB100 revealed that the diversity of oligosaccharide was distinct at each site. These data provide information to understand the role of oligosaccharides of apoB100 in LDL particles

Materials and methods

Materials

Acetonitrile, formic acid, chymotrypsin, and guanidine hydrochloride were from Wako Pure Chemicals (Osaka, Japan). Tosylphenylalanine chloromethane (TPCK)-treated trypsin was from Sigma (St. Louis, MO). Human apoB100 was purchased from MP Biomedicals (Irvine, CA). This product is derived from pooled human plasma, which is not particularly high-fat plasma. The water used was obtained from a Milli-Q water system (Millipore, Bedford, MA). All other reagents were of the highest quality available.

Reduction and S-carboxymethylation of apoB100

ApoB100 (500 µg) was dissolved in 810 µl of 0.5 M Tris–HCl buffer (pH 8.5) that contained 8 M guanidine hydrochloride and 5 mM ethylenediamine tetra-acetic acid. After the addition of 6 µl 2-mercaptoethanol, the mixture was incubated for 2 h at 40°C. Then, 17 mg of monoiodoacetic acid was added, and the resulting mixture was incubated for 2 h at 40°C in the dark. The reaction mixture was applied to a PD-10 column (Amersham Pharmacia Biotech, Uppsala, Sweden) to remove the reagents, and the eluate was lyophilized.

Enzyme digestion of apoB100

Reduced and carboxymethylated apoB100 was redissolved in 500 µl 0.1 M Tris–HCl buffer (pH 8.0). Half of the reduced and carboxymethylated apoB100 was incubated with 0.02 µg/µl of TPCK-treated trypsin (1:50 w/w) for 2 h at 37°C and the rest was incubated with 0.04 µg/µl of chymotrypsin (1:25 w/w) for 72 h at 37°C. The enzyme digestions were stopped by storing at −20°C before analysis.

High-performance LC of trypsin or chymotrypsin-digested apoB100

Tryptic digest (4 µg, about 8 pmol) and chymotryptic digest (2 µg, about 4 pmol) were analyzed by LC/ESI MS/MS. High-performance LC was performed on a Paradigm MS 4 equipped with a Magic C18 column (0.2 × 50 mm, Michrome BioResources, Auburn, CA). The eluents consisted of water containing 2% (v/v) acetonitrile and 0.1% (v/v) formic acid (pump A) and 90% acetonitrile and 0.1% formic acid (pump B). Trypsin- or chymotrypsin-digested samples of apoB100 were eluted with 5% B for 10 min, followed by a liner gradient from 5% to 70% of pump B in 130 min at a flow rate of 2 µl/min.

ESI Q-TOF MS/MS

MS analyses were performed using a QSTAR Pulsar i quadrupole TOF mass spectrometer (AB/MDS Sciex, Toronto, Canada) equipped with a nano-electrospray ion source. The mass spectrometer was operated in the positive ion mode. The nanospray voltage was set at 2500 V. Mass spectra for MS analysis were acquired over *m/z* 1000–2000 and 700–2000 for tryptic and chymotryptic digests, respectively, and for MS/MS analysis, over *m/z* 100–2000. After every regular MS acquision, MS/MS acquision was performed against multiple charged ions. The molecular ions were selected by data-dependent acquiring in the quadrupole analyzer and fragmented in the hexapole collision cell. The collision energy was varied between 40 and 80 eV depending on the size and charge of the molecular ion. All signals were monoisotopically resolved. Accumulation time of spectra is 1.0 and 2.0 s for MS and MS/MS, respectively.

Acknowledgments

We thank Dr. Nishimaki-Mogami for helpful suggestions. This study was supported by a grant-in-aid for Research on Health Sciences focusing on Drug Innovation from the Japan Health Sciences Foundation.

Abbreviations

apoB100, apolipoprotein B100; ESI, electrospray ionization; LC, liquid chromatography; LDL, low-density lipoprotein; MS, mass spectrometry; TIC, total ion chromatogram; TOF, time of flight; TPCK, Tosylphenylalanine chloromethane; VLDL, very low-density lipoprotein.

References

Attie, A.D., Weinstein, D.B., Freeze, H.H., Pittman, R.C., and Steinberg, D. (1979) Unaltered catabolism of desialylated low-density lipoprotein in the pig and in cultured rat hepatocytes. *Biochem. J.*, **180**, 647–654.

Boren, J., Lee, I., Zhu, W., Arnold, K., Taylor, S., and Innerarity, T.L. (1998) Identification of the low density lipoprotein receptor-binding site in apolipoprotein B100 and the modulation of its binding activity by the carboxyl terminus in familial defective apo-B100. *J. Clin. Invest.*, **101**, 1084–1093.

Carr, S.A., Huddleston, M.J., and Bean, M.F. (1993) Selective identification and differentiation of *N*- and *O*-linked oligosaccharides in glycoproteins by liquid chromatography-mass spectrometry. *Protein Sci.*, **2**, 183–196.

Chen, S.H., Yang, C.Y., Chen, P.F., Setzer, D., Tanimura, M., Li, W.H., Gotto, A.M. Jr, and Chan, L. (1986) The complete cDNA and amino acid sequence of human apolipoprotein B-100. *J. Biol. Chem.*, **261**, 12918–12921.

Duffin, K.L., Welply, J.K., Huang, E., and Henion, J.D. (1992) Characterization of *N*-linked oligosaccharides by electrospray and tandem mass spectrometry. *Anal. Chem.*, **64**, 1440–1448.

Filipovic, I., Schwarzmann, G., Mraz, W., Wiegandt, H., and Buddecke, E. (1979) Sialic-acid content of low-density lipoproteins controls their binding and uptake by cultured cells. *Eur. J. Biochem.*, **93**, 51–55.

Fujioka, Y., Taniguchi, T., Ishikawa, Y., and Yokoyama, M. (2000) Significance of acidic sugar chains of apolipoprotein B-100 in cellular metabolism of low-density lipoproteins. *J. Lab. Clin. Med.*, **136**, 355–362.

Garner, B., Harvey, D.J., Royle, L., Frischmann, M., Nigon, F., Chapman, M.J., and Rudd, P.M. (2001) Characterization of human apolipoprotein B100 oligosaccharides in LDL subfractions derived from normal and hyperlipidemic plasma: deficiency of alpha-*N*-acetylneuraminyllactosyl-ceramide in light and small dense LDL particles. *Glycobiology*, **11**, 791–802.

Kawasaki, N., Ohta, M., Itoh, S., and Hayakawa, T. (2004) Analyses of glycopeptides and glycoproteins by liquid chromatography-mass spectrometry and liquid chromatography-tandem mass spectrometry. *Methods Mol. Biol.*, **251**, 263–274.

Knott, T.J., Pease, R.J., Powell, L.M., Wallis, S.C., Rall, S.C. Jr, Innerarity, T.L., Blackhart, B., Taylor, W.H., Marcel, Y., Milne, R., and others. (1986) Complete protein sequence and identification of structural domains of human apolipoprotein B. *Nature*, **323**, 734–738.

Law, S.W., Grant, S.M., Higuchi, K., Hospattankar, A., Lackner, K., Lee, N., and Brewer, H.B. Jr. (1986) Human liver apolipoprotein B-100 cDNA: complete nucleic acid and derived amino acid sequence. *Proc. Natl Acad. Sci. USA*, **83**, 8142–8146.

Ling, V., Guzzetta, A.W., Canova-Davis, E., Stults, J.T., Hancock, W.S., Covey, T.R., and Shushan, B.I. (1991) Characterization of the tryptic map of recombinant DNA derived tissue plasminogen activator by high-performance liquid chromatography-electrospray ionization mass spectrometry. *Anal. Chem.*, **63**, 2909–2915.

Orekhov, A.N., Tertov, V.V., Mukhin, D.N., and Mikhailenko, I.A. (1989) Modification of low density lipoprotein by desialylation causes lipid accumulation in cultured cells: discovery of desialylated lipoprotein with altered cellular metabolism in the blood of atherosclerotic patients. *Biochem. Biophys. Res. Commun.*, **162**, 206–211.

Segrest, J.P., Jones, M.K., Mishra, V.K., Anantharamaiah, G.M., and Garber, D.W. (1994) ApoB-100 has a pentapartite structure composed of three amphipathic alpha-helical domains alternating with two amphipathic beta-strand domains. Detection by the computer program LOCATE. *Arterioscler Thromb.*, **14**, 1674–1685.

Shireman, R.B. and Fisher, W.R. (1979) The absence of a role for the carbohydrate moiety in the binding of apolipoprotein B to the low density lipoprotein receptor. *Biochim. Biophys. Acta*, **572**, 537–540.

Taniguchi, T., Ishikawa, Y., Tsunemitsu, M., and Fukuzaki, H. (1989) The structures of the asparagine-linked sugar chains of human apolipoprotein B-100. *Arch. Biochem. Biophys.*, **273**, 197–205.

Vukmirica, J., Nishimaki-Mogami, T., Tran, K., Shan, J., McLeod, R.S., Yuan, J., and Yao, Z. (2002) The N-linked oligosaccharides at the amino terminus of human apoB are important for the assembly and secretion of VLDL. *J. Lipid. Res.*, **43**, 1496–1507.

Yang, C.Y., Chen, S.H., Gianturco, S.H., Bradley, W.A., Sparrow, J.T., Tanimura, M., Li, W.H., Sparrow, D.A., DeLoof, H., Rosseneu, M., and others. (1986) Sequence, structure, receptor-binding domains and internal repeats of human apolipoprotein B-100. *Nature*, **323**, 738–742.

Yang, C.Y., Gu, Z.W., Weng, S.A., Kim, T.W., Chen, S.H., Pownall, H.J., Sharp, P.M., Liu, S.W., Li, H.W., Gotto, A.M. Jr., and Chan, L. (1989) Structure of apolipoprotein B-100 of human low density lipoproteins. *Arteriosclerosis*, **9**, 96–108.

REGULAR ARTICLE

Glycomic/glycoproteomic analysis by liquid chromatography/mass spectrometry: Analysis of glycan structural alteration in cells

Noritaka Hashii, Nana Kawasaki, Satsuki Itoh, Mashashi Hyuga, Toru Kawanishi and Takao Hayakawa

Division of Biological Chemistry and Biologicals, National Institute of Health Sciences, Tokyo

The alteration of glycosyltransferase expression and the subsequent changes in oligosaccharide structures are reported in several diseases. The analysis of glycan structural alteration in glycoproteins is becoming increasingly important in the discovery of therapies and diagnostic markers. In this study, we propose a strategy for glycomic/glycoproteomic analysis based on oligosaccharide profiling by LC/MS followed by proteomic approaches, including 2-DE and 2-D lectin blot. As a model of aberrant cells, we used Chinese hamster ovary cells transfected with *N*-acetylglucosaminyltransferase III (GnT-III), which catalyzes the addition of a bisecting *N*-acetylglucosamine (GlcNAc) to β-mannose of the mannosyl core of *N*-linked oligosaccharides. LC/MS equipped with a graphitized carbon column (GCC) enabled us to elucidate the structural alteration induced by the GnT-III expression. Using 2-D lectin blot followed by LC/MS/MS, the protein carrying an extra *N*-acetylhexosamine in cells transfected with GnT-III was successfully identified as integrin α3. Thus, oligosaccharide profiling by GCC-LC/MS followed by proteomic methods can be a powerful tool for glycomic/glycoproteomic analysis.

Received: September 20, 2004
Revised: April 22, 2005
Accepted: April 22, 2005

Keywords:
2DE / LC/MS / Lectin blotting / Oligosaccharides profiling

1 Introduction

It is common knowledge that approximately 50% of proteins in mammalian cells are glycosylated and that glycans play crucial roles in various biological events including cell recognition [1], adhesion [2] and cell-cell interaction [3]. The alteration of glycosyltransferase expression and subsequent changes in oligosaccharide structures are reported in several diseases, including inherited diseases [4], the progression of cancer [5] and autoimmune diseases [6–8]. The analysis of glycan structural alteration in glycoproteins is becoming increasingly important in the discovery of therapies and diagnostic markers.

Comprehensive analysis of proteins in a given cellular sample is the most effective means of elucidating the disease mechanism. Simultaneous separation and characterization of proteins by 2-DE and 2-D LC followed by MS have been utilized as the fundamental approaches to proteomic analysis; however, these approaches alone are ineffectual for the elucidation of the glycan structural alteration in glycoproteins. A strategy based on qualitative and quantitative glycomic analysis is necessary for the study of glycosylation-associated diseases.

LC/MS is widely used for glycosylation analysis in glycoproteins. Previously, we demonstrated that LC/MS equipped with a graphitized carbon column (GCC-LC/MS) is a useful means of oligosaccharide profiling and for the structural analysis of carbohydrates [9–12]. Using this method, oligosaccharides, including high mannose, hybrid and complex

Correspondence: Dr. Nana Kawasaki, 1–18–1, Kamiyoga, Setagaya-ku, Tokyo, 158–8501, Japan
E-mail: nana@nihs.go.jp
Fax: +81-3-3700-9084

Abbreviations: CHO, Chinese hamster ovary; **CHO-III cells**, CHO cells transfected with *N*-acetylglucosaminyltransferase III; **dHex**, deoxyhexose; **GCC**, graphitized carbon column; **GlcNAc**, *N*-acetylglucosamine; **GnT-III**, *N*-acetylglucosaminyltransferase III; **Hex**, hexose; **HexNAc**, *N*-acetylhexosamine; **NeuAc**, *N*-acetylneuraminic acid; **PNGase F**, peptide *N*-glycosidase F

© 2005 WILEY-VCH Verlag GmbH & Co. KGaA, Weinheim

types with or without sialic acids, can be separated, and structural information can be obtained from their mass spectra and chromatographic behavior.

Here we propose a strategy for performing glycomic/glycoproteomic analysis based on a combination of GCC-LC/MS and proteomic approaches.

First, GCC-LC/MS is applied to the analysis of oligosaccharide structural alteration in aberrant cells. Chinese hamster ovary (CHO) cells, used as a model of aberrant cells, were transfected with *N*-acetylglucosaminyltransferase III (GnT-III), which catalyzes the addition of bisecting *N*-acetylglucosamine (GlcNAc) to the trimannosyl core of *N*-linked oligosaccharides [13] and is associated with cell adhesion [14] and the suppression of tumor cell metastasis [15–17]. Then, 2-D lectin blotting followed by LC/MS/MS was used to identify the protein in which glycosylation was altered by the expression of GnT-III.

2 Materials and methods

2.1 Cell lines and culture

The CHO cells were obtained from the Japanese Collection of Research Bioresources (Tokyo, Japan). The human GnT-III cDNA was cloned into the pCI-neo vector. The expression vector was transfected into CHO cells with LipofectAMINE plus reagent, according to the manufacturer's instructions. To screen the transformants, the transfectants were cultured with Ham's F12 medium supplemented with 10% fetal calf serum (FCS) and 1 mg/mL G418. After 2 weeks, the colonies were lifted with a micropipette. A high GnT-III-expressing clone was used in succeeding experiments.

The CHO cells and GnT-III-transfected CHO cells (CHO-III cells) were cultured in Ham's F12 medium supplemented with 10% FCS, 100 U/mL of penicillin and 100 μg/mL of streptomycin under a humidified atmosphere of 95% air and 5% CO_2. After harvesting CHO and CHO-III cells, they were rinsed with PBS containing protease inhibitors and 2 mM EDTA.

2.2 Preparation of insoluble and soluble fractions

The insoluble and soluble fractions were prepared from CHO and CHO-III cells using a Mem-PER Eukaryotic Membrane Protein Extraction Reagent Kit (Pierce Biotechnology, P.O., USA). The detergent in these fractions was removed with Detergent-OUT (Geno Technology, M.O., USA) three times. For desalting and degreasing, seven volumes of acetone were added to the sample solution, and the mixture was stirred and sonicated. The mixture was then incubated at −20°C for 1 h and centrifuged at 4°C for 15 min, 15 000 × g. The supernatants were discarded, and the pellets dried. The protein concentrations were determined using a BCA protein assay kit (Pierce).

2.3 Preparation of *N*-linked oligosaccharide alditols

The protein (500 μg) from each fraction was dissolved in 810 μL of 0.5 M Tris-HCl containing 8 M guanidine-HCl and 5 mM EDTA (pH 8.6), and then 6.0 μL of 2-mercaptoethanol were added in the solution. After incubation at room temperature for 2 h, freshly prepared 0.6 M sodium monoiodoacetamide (135 μL) was added to the solution. After incubation at room temperature for 2 h in the dark, the solution was desalted with PD10 column (Amersham Biosciences, NJ, USA), and the elute was lyophilized. The carboxylmethylated proteins were dissolved in 500 μL of 100 mM PBS (pH 7.2), and 20 U of peptide *N*-glycosidase F (PNGase F) (Roche Diagnostics, Mannheim, Germany) were added to the solution. After incubation at 37°C for 4 days, 1.74 mL of cold ethanol was added to the solution, the mixture was incubated at −20°C for 3 h, and proteins were removed by centrifugation at 4°C for 10 min (15 000 × g). The supernatants containing oligosaccharides were evaporated, and then lyophilized. The oligosaccharides were incubated with 500 μL of 0.5 M $NaBH_4$ at room temperature for 16 h, and then neutralized with 10% (v/v) acetic acid to pH 6.5 and desalted with Envi-Carb (Supelco, Bellefonte, USA).

2.4 GCC-LC/MS

LC was carried out using a MAGIC 2002 system (Michrom BioResources, Auburn, CA, USA). The GCC used was a Hypercarb column (150 × 0.2 mm, ThermoFinnigan, San Jose, CA, USA). The eluents were 5 mM ammonium acetate, pH 8.5, containing 2% ACN (pump A) and 5 mM ammonium acetate, pH 8.5, containing 80% ACN (pump B). The borohydride-reduced oligosaccharides were eluted at a flow rate of 2 μL/min with a gradient of 10–45% of pump B in 90 min. Mass spectra were recorded on a TSQ 7000 triple-stage quadruple mass spectrometer (ThermoFinnigan) equipped with a nanoelectorospray ion source (AMR, Inc., Tokyo, Japan). The mass spectrometer was operated in positive ion mode. Ions in the range of m/z 900–2400 were acquired with a scan duration of 3 s. The ESI voltage was set at 2.0 kV, and the capillary temperature was 175°C. The electron multiplier was set at 1.0 kV. Collisions for MS/MS were carried out with collision energy of 25%, scan duration of 4 s., and mass range of m/z 100–2000.

2.5 1-D SDS-PAGE and lectin blotting

Proteins were separated by 1-D SDS-PAGE (12.5% T, 3% C) as described by Laemmli [18] and stained with SYPRO Orange (Bio-Rad, Richmond, CA, USA) at room temperature for 30 min in transfer buffer (25 mM Tris-HCl, 20 mM glycine and 20% methanol). The gel images were scanned on a Tyhoon 9400 (Amersham Biosciences) at an excitation wavelength of 540/25 nm and an emission wavelength of 590/30 nm. After saving the gel image, the proteins were blotted to a PVDF membrane (Immun-Blot PVDF membrane,

© 2005 WILEY-VCH Verlag GmbH & Co. KGaA, Weinheim

0.2 μm, Bio-Rad) at 3.0 mA/cm^2, 20 V for 30 min in transfer buffer containing 0.1% SDS using a semi-dry blotter (Trans-blot SD sel, Bio-Rad). The efficiency and position of the transfer were confirmed using SYPRO Orange transferred together with proteins. Nonspecific sites on the membrane were blocked at 4°C for 16 h in 0.5% casein-PBS. After the membranes were washed with 0.05% Tween-PBS (T-PBS) three times, they were treated with 0.1 U/mL of sialidase (Nacalai Tesque, Kyoto, Japan) at 37°C for 16 h in 0.5 M acetate buffer (pH 5.0). The membranes were then re-blocked with 0.5% casein-PBS at 37°C for 15 min, washed with T-PBS three times, and incubated with biotinylated phytohemagglutinin-E4 (PHA-E4, 2 μg/mL) at 4°C for 2 h in PBS (pH 7.4). The membranes were then washed with T-PBS and incubated with 1:1000 diluted avidin-alkaline phosphatase (AP) complex solution at 4°C for 1 h in PBS.

2.6 Concentration of target proteins in the gel

The band detected by lectin blotting on 1-D gel was excised and then mashed in 20 mM Tris-HCl (pH 8.0) containing 2% SDS. The proteins in the gel particles were extracted by intermittent sonication at 4°C for 30 min, followed by shaking at room temperature for 16 h. After extraction, the gel particles were removed by centrifugation (15 000 × g). The proteins in the supernatant were precipitated with sevenfold acetone at −20°C for 3 h, and then the precipitates were washed with acetone three times to remove salts and detergent.

2.7 2-DE

For first dimension IEF of the sample, Immobiline DryStrip gel (13 cm, pH4–7 NL, Amersham Biosciences) was used. The samples were dissolved in IEF solution containing 7 M urea, 2 M thiourea, 18 mM DTT, 0.5% IPG buffer, 2% CHAPS, and bromophenol blue. Dried IPG strips were rehydrated overnight in the sample solution. IEF was then performed using the following steps: 500 V for 1 h, 100 V for 1 h, and 8000 V for 2 h, *i.e.* a total of 17.5 kVh.

IPG strips were treated with 10 mL of 50 mM Tris-HCl (pH 8.8) containing 2% SDS, 6 M urea, 30% glycerol and 65 mM DTT for 15 min, and then treated with 10 mL of 50 mM Tris-Cl (pH 8.8) containing 2% SDS, 6 M urea, 30% glycerol and 135 mM iodoacetamide for 15 min in order to reduce the disulfide bonds of cysteinyl residues. SDS-polyacrylamide gels (7.5%T, 3%C, size 140 × 140 × 1 mm) and running buffer containing 25 mM Tris-HCl, 192 mM glycine and 0.1% SDS were used for the 2-DE. The gels were run at 25 mA/gel after setting the IPG strip on the gel. Fluorescent staining and scanning of gel, followed by lectin blotting, were performed as mentioned above. In 2-D lectin blotting, the proteins were blotted to a PVDF membrane at 3.0 mA/cm^2, 20 V for 90 min.

2.8 In-gel digestion and protein identification by LC/MS/MS

Interesting spots were excised from the 2-DE gel for in-gel trypsin digestion. The gel particles were destained with 20 mM ammonium bicarbonate containing 50% methanol in microcentrifuge tubes, and dehydrated in 100% ACN. Enzymatic digestion was performed overnight at 37°C with 5 μL of 20 μg/mL trypsin (Promega, Madison, WI, USA) in 20 mM ammonium bicarbonate (pH 8.5). Digested peptides were extracted with 1% TFA in 50% ACN, and samples were dried with a Speed-Vac and redissolved in 0.1% TFA for LC/MS.

LC was carried out using a Paradigm MS4 (Michrom BioResources) equipped with Magic C18 column (50 × 0.2 mm, Michrom BioResources). The eluents were 0.1% formic acid containing 2% ACN (pump A), and 0.1% formic acid containing 90% ACN (pump B). The peptides were eluted at a flow rate of 2 μL/min with a gradient of 5–70% of pump B in 30 min. Mass spectra were recorded on an API QSTAR Pulsar i (Applied Biosystems, Foster City, CA, USA) in the positive ion mode. The proteins were identified by searching the Swiss-Prot database using MASCOT (Matrix Science, UK). The mass range and MS/MS range were *m/z* 400–2000 and *m/z* 100–2000, respectively, and the ESI voltage was set at 2.5 kV.

3 Results

3.1 Analysis of glycans in the insoluble fractions

N-linked oligosaccharides were released from soluble and insoluble fractions by PNGase F and reduced with $NaBH_4$ to prevent the separation of anomers by GCC. Figure 1A shows the *N*-linked oligosaccharide profile of the insoluble fraction from CHO cells (5 × 10^7). Diverse oligosaccharide ions were detected by full scan in the positive ion mode of MS. Oligosaccharides were numbered with the labels on peaks where they were detected, and the multiple oligosaccharides in single peak were classified by the digits behind alphabets, such as peaks A1 and A2. Their monosaccharide compositions were deduced from the *m/z* values as shown in Table 1. *N*-linked oligosaccharides from CHO cells have a high proportion of high mannose-type and bi-, tri- and tetra-antennary complex type oligosaccharides [19, 20]. High mannose-type oligosaccharides, $[Man]_{5-9}[GlcNAc]_2$ were detected at 9–23 min (peaks A–E and K). Major components (peaks N2, Q2, R1, S1, T1, U1 and V2) were deduced as fucosylated and non-fucosylated biantennary forms with mono- and di-sialic acids from previous articles and their monosaccharide compositions. Various oligosaccharides, including mono- (peak N1 and Q1), tri- (peak P1, U2, V1), tetra-antennary (peak V3), and hybrid-type (peak F1 and I1) oligosaccharides were detected as minor components together with low molecular weight oligosaccharides such as the trimannosyl core (peaks G1 and O1).

© 2005 WILEY-VCH Verlag GmbH & Co. KGaA, Weinheim

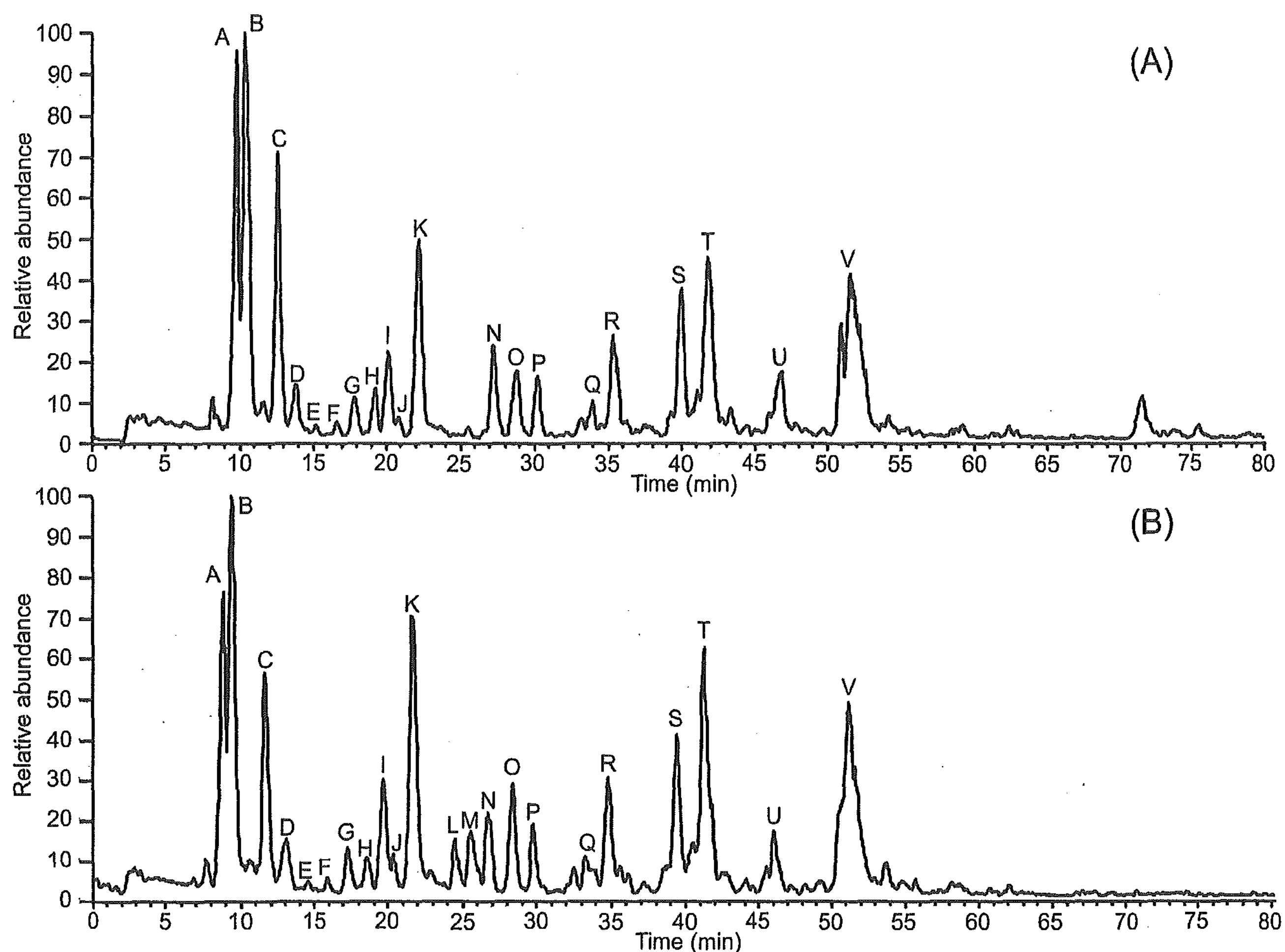

Figure 1. Total ion chromatograms of GCC-LC/MS of borohydride-reduced *N*-linked oligosaccharides released from insoluble fraction of CHO (A) and CHO-III (B) in positive ion mode. Pump A: 5 mM ammonium acetate, pH 8.5, containing 2% ACN. Pump B: 5 mM ammonium acetate, pH 8.5, containing 80% ACN. The borohydride-reduced oligosaccharides were eluted at a flow rate of 2 μL/min with a gradient of 10–45% of pump B in 90 min.

Figure 1B shows the oligosaccharide profile of the CHO-III-insoluble fraction. The distribution of oligosaccharides in CHO-III was different from that in the CHO cell insoluble fraction. Some additional peaks (peaks L1 and M1) were detected in the CHO-III-insoluble fraction, and their doubly charged ions at m/z 1143.2 and 1143.0 were consistent with the theoretical m/z values of fucosylated biantennary-bearing NeuAc with one additional HexNAc. Figure 2 shows the MS/MS spectrum of peak M1. Detection of $B_{1\gamma}/Y_6^{2+}$ at m/z 894.1 and an intense ion of $[HexNAc]^+$, at m/z 204 suggest that the oligosaccharide (peak M1) carries one GlcNAc at either of the non-reducing ends. Peak M1 is possibly assigned to bisected biantennary form. In addition, peaks D1, I2 and S2, which were not found in the profile of CHO, were detected in that of CHO-III (Fig. 1B). They can also be deduced as bisected biantennary forms from their MS/MS spectra. Other than these oligosaccharides bearing GlcNAc at either of the non-reducing ends in CHO-III cells, there was no significant difference in glycosylation between CHO and CHO-III cells. These results suggest that only limited oligosaccharides are altered by the expression of GnT-III.

3.2 Analysis of glycans in the soluble fractions

Figure 3A and B shows the *N*-linked oligosaccharide profiles of the soluble fractions of CHO and CHO-III, respectively. The oligosaccharide components of soluble fractions are very different from those of insoluble fractions (Table 1). High mannose-type oligosaccharides, $[Man]_{5-9}[GlcNAc]_2$, were detected as major components (peaks A–C and K), and complex-type and hybrid-type oligosaccharides were detected as minor oligosaccharides in the soluble fraction. Oligosaccharides bearing extra GlcNAc (D1, L1 and M1) were also detected in the soluble fraction of CHO-III.

© 2005 WILEY-VCH Verlag GmbH & Co. KGaA, Weinheim

Table 1. Observed *m/z* values and carbohydrate compositions of peaks A-V in total ion chromatogram 3 of CHO-insoluble (Fig. 1A), CHO-III-insoluble (Fig. 1B), CHO-soluble (Fig. 3A) and CHOIII-soluble (Fig. 3B) fractions

Carbohydrate composition[a]	Theoretical mass[b]	Peak No.		Insoluble fraction				Soluble fraction			
				CHO		CHO-III		CHO		CHO-III	
				Charge state	Observed *m/z*	Charge state	Observed *m/z*	Charge state	Observed *m/z*	Charge state	Observed *m/z*
$[Hex]_7[HexNAc]_2$	1561.4	A	A1	H^+	1562.2	H^+	1562.0	Na^+	1584.4	Na^+	1584.2
$[Hex]_8[HexNAc]_2$	1723.5		A2	Na^+	1746.3	Na^+	1746.3	Na^+	1746.5	Na^+	1746.1
$[Hex]_9[HexNAc]_2$	1885.7	B	B1	Na^+	1908.4	Na^+	1908.5	Na^+	1908.4	Na^+	1908.9
$[Hex]_6[HexNAc]_2$	1399.3	C	C1	H^+	1400.1	H^+	1400.0	H^+	1399.7	H^+	1399.9
$[Hex]_7[HexNAc]_2$	1561.4		C2	Na^+	1584.2	Na^+	1584.0	Na^+	1584.8	Na^+	1584.0
$[dHex]_1[Hex]_5[HexNAc]_5$	1992.9	D	D1		N.D.[c]	$2H^+$	**997.4**		N.D.	$2H^+$	**997.5**
$[Hex]_6[HexNAc]_2$	1399.3		D2	Na^+	1422.0	Na^+	1421.9		N.D.		N.D.
$[Hex]_7[HexNAc]_2$	1561.4		D3	Na^+	1584.2	Na^+	1584.1		N.D.		N.D.
$[Hex]_8[HexNAc]_2$	1723.5		D4	Na^+	1746.2	Na^+	1746.4		N.D.		N.D.
$[Hex]_4[HexNAc]_2$	1075.0	E	E1	Na^+	1097.9	Na^+	1097.6		N.D.		N.D.
$[Hex]_6[HexNAc]_2$	1399.3		E2	H^+	1400.1	H^+	1400.0		N.D.		N.D.
$[Hex]_6[HexNAc]_3$	1602.5	F	F1	H^+	1604.0	H^+	1603.1		N.D.		N.D.
$[Hex]_3[HexNAc]_2$	912.8	G	G1	H^+	913.7	H^+	913.7	Na^+	935.7	Na^+	935.6
$[Hex]_5[HexNAc]_4$	1643.5	H	H1	H^+	1644.5	H^+	1644.2	Na^+	1666.3	Na^+	1666.4
$[Hex]_6[HexNAc]_4$	1827.6	I	I1	$2Na^+$	914.7	$2Na^+$	914.7		N.D.		N.D.
$[Hex]_5[HexNAc]_5[NeuAc]_1$	2137.9		I2		N.D.	$2H^+$	**1069.8**		N.D.		N.D.
$[dHex]_1[Hex]_3[HexNAc]_4$	1465.4	J	J1	H^+	1466.1	H^+	1466.1	Na^+	1488.2	Na^+	1487.9
$[Hex]_5[HexNAc]_2$	1237.1	K	K1	H^+	1238.0	H^+	1238.0	H^+	1237.9	H^+	1237.9
$[dHex]_1[Hex]_5[HexNAc]_5[NeuAc]_1$	2284.1	L	L1		N.D.	$2H^+$	**1143.2**		N.D.	$2H^+$	**1142.9**
$[dHex]_1[Hex]_5[HexNAc]_5[NeuAc]_1$	2284.1	M	M1		N.D.	$2H^+$	**1143.0**		N.D.	$2H^+$	**1143.3**
$[dHex]_1[Hex]_4[HexNAc]_3$	1424.3	N	N1	H^+	1425.4	H^+	1425.3	Na^+	1447.1	Na^+	1447.1
$[dHex]_1[Hex]_5[HexNAc]_4$	1789.7		N2	H^+	1790.1	H^+	1790.3	Na^+	1812.3	Na^+	1812.1
$[dHex]_1[Hex]_3[HexNAc]_2$	1059.0	O	O1	H^+	1059.7	H^+	1059.7	H^+	1059.8	H^+	1059.7
$[dHex]_1[Hex]_6[HexNAc]_5$	2155.0	P	P1	$2H^+$	1078.5	$2H^+$	1078.5		N.D.		N.D.
$[dHex]_1[Hex]_3[HexNAc]_3$	1262.2	Q	Q1	H^+	1263.0	H^+	1263.0		N.D.		N.D.
$[Hex]_5[HexNAc]_4[NeuAc]_1$	1934.7		Q2	$2H^+$	968.4	$2H^+$	968.4		N.D.		N.D.
$[Hex]_5[HexNAc]_4[NeuAc]_1$	1934.7	R	R1	$2H^+$	968.4	$2H^+$	968.4	$2H^+$	968.7	$2H^+$	968.2
$[dHex]_1[Hex]_5[HexNAc]_4[NeuAc]_1$	2080.9	S	S1	$2H^+$	1041.4	$2H^+$	1041.4	$2H^+$	1041.4	$2H^+$	1041.3
$[dHex]_1[Hex]_5[HexNAc]_5[NeuAc]_2$	2574.0		S2		N.D.	$2H^+$	**1288.5**		N.D.		N.D.
$[dHex]_1[Hex]_5[HexNAc]_4[NeuAc]_1$	2080.9	T	T1	$2H^+$	1041.4	$2H^+$	1041.5	$2H^+$	1041.4	$2H^+$	1041.3
$[Hex]_5[HexNAc]_4[NeuAc]_2$	2226.0	U	U1	$2H^+$	1114.0	$2H^+$	1113.9	$2H^+$	1113.9	$2H^+$	1113.9
$[dHex]_1[Hex]_6[HexNAc]_5[NeuAc]_1$	2446.2		U2	$2H^+$	1224.2	$2H^+$	1224.3	$2Na^+$	1124.9		N.D.
$[dHex]_1[Hex]_6[HexNAc]_5[NeuAc]_2$	2737.5	V	V1	$2H^+$	1370.0	$2H^+$	1370.0		N.D.		N.D.
$[dHex]_1[Hex]_5[HexNAc]_4[NeuAc]_2$	2372.1		V2	$2H^+$	1187.1	$2H^+$	1187.1	$2H^+$	1187.2	$2H^+$	1187.2
$[dHex]_1[Hex]_7[HexNAc]_6[NeuAc]_1$	2811.6		V3	$2H^+$	1406.8	$2H^+$	1406.6		N.D.		N.D.

The characteristic *m/z* values observed in total ion chromatograms of CHO-III are depicted in bold type.

a) [dHex], deoxyhexose; [Hex], hexose; [HexNAc], *N*-acetylhexosamine; [NeuAc], *N*-acetylneuraminic acid.

b) Monoisotopic mass values.

c) Not detected.

© 2005 WILEY-VCH Verlag GmbH & Co. KGaA, Weinheim

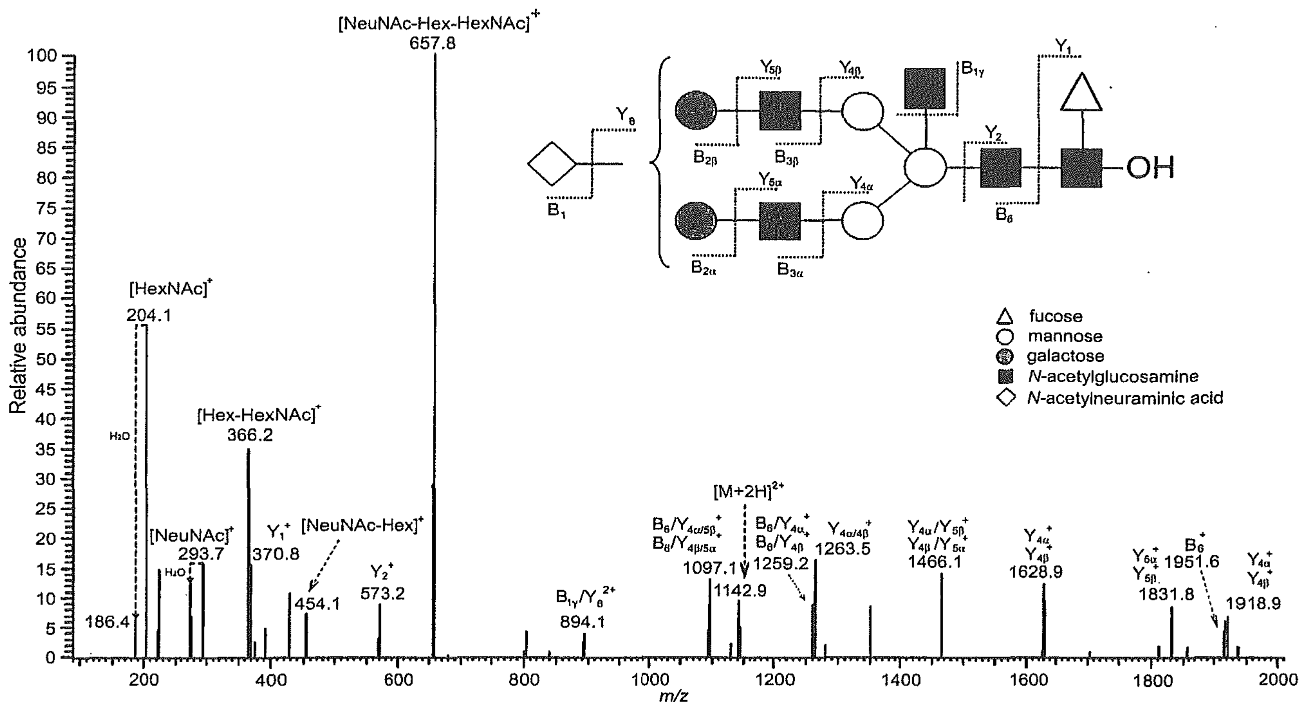

Figure 2. MS/MS spectrum of fucosylated biantennary *N*-linked oligosaccharide (peak M1) detected in the insoluble fraction from CHO-III.

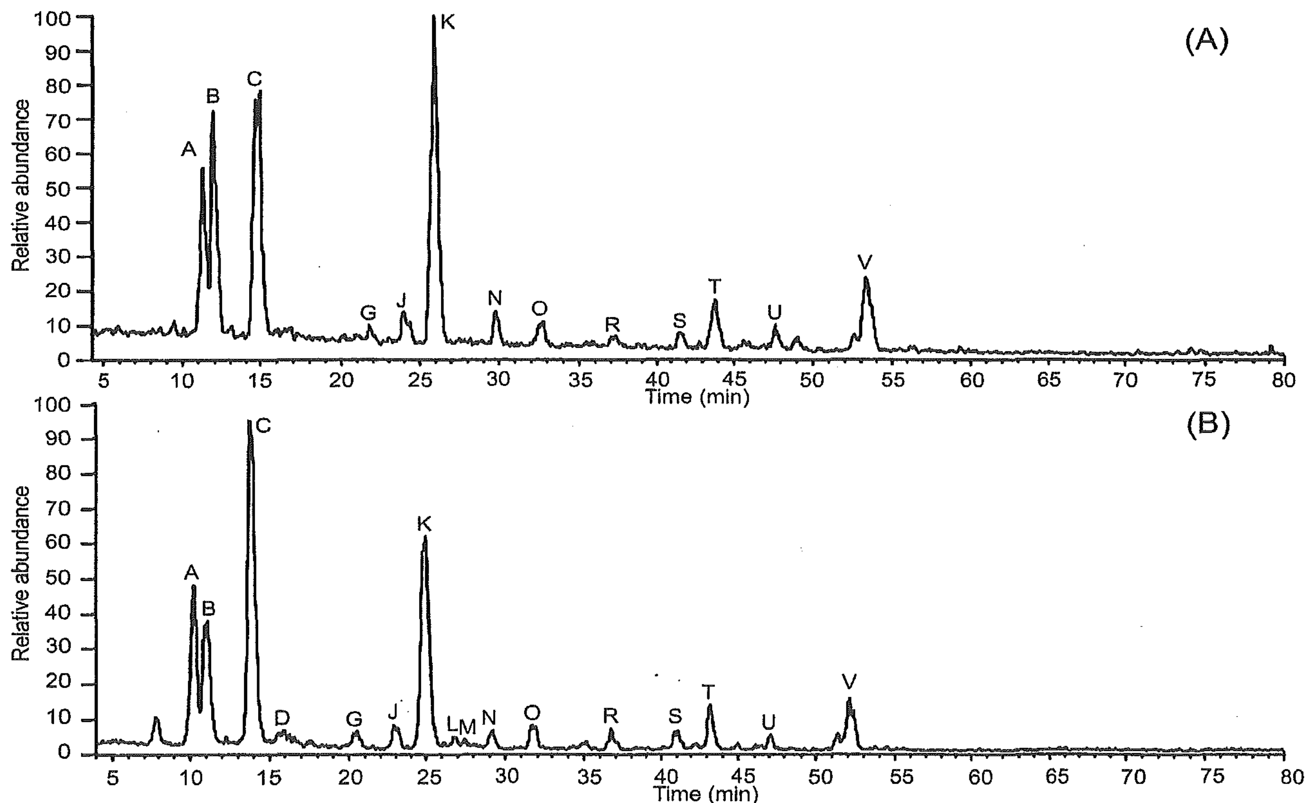

Figure 3. Total ion chromatograms of GCC-LC/MS of borohydride-reduced *N*-linked oligosaccharides released from the soluble fractions of CHO (A) and CHO-III (B) in positive ion mode. Pump A: 5 mM ammonium acetate, pH 8.5, containing 2% ACN. Pump B: 5 mM ammonium acetate, pH 8.5, containing 80% ACN. The borohydride-reduced oligosaccharides were eluted at a flow rate of 2 μL/min with a gradient of 10–45% of pump B in 90 min.

© 2005 WILEY-VCH Verlag GmbH & Co. KGaA, Weinheim

3.3 Identification of protein bearing bisected oligosaccharides

To identify proteins with altered glycans by the expression of GnT-III, we performed 2-DE followed by lectin blotting using PHA-E4 lectin, which recognizes bisecting GlcNAc in complex-type oligosaccharides. Although some bisected glycoproteins (70–120 kDa) could be visualized by 2-D lectin blotting, their expressions were too low to be detected on 2-DE gel. Lectin affinity chromatography, which is generally used for the concentration of glycoproteins, cannot be used for the insoluble fraction due to the presence of detergent in the solvent medium. Therefore, we first performed 1-D SDS-PAGE followed by lectin blotting, and then proteins in the range of 70–120 kDa were extracted from the gel (Fig. 4). 2-DE followed by lectin blotting was then performed, and interesting spots were successfully detected on 2-DE gel. Figure 5A and B shows the 2-DE gel images and the 2-D lectin blot of extracted proteins, respectively. The remarkable train spots (120 Da) of glycoprotein were picked up and in-gel digested with trypsin. The digest was subjected to LC/MS/MS, and the integrin α3 precursor was identified as the GnT-III target protein.

4 Discussion

The development of a simple and rapid method to explore glycan structural alteration in a complex mixture is required to elucidate the mechanisms of diseases involving glycan alteration. In this study, we demonstrated that GCC-LC/MS, which is used for glycosylation analysis in glycoproteins, is applicable for the exploration of changes in glycosylation between samples. Using GCC-LC/MS, high mannose, hybrid, and complex types as well as neutral and acidic oligosaccharides could be separated and characterized by a single analysis. GCC-LC/MS clearly shows differences in glycosylation between soluble and insoluble fractions. High mannose-type oligosaccharides were detected as major components in the soluble fraction. The soluble fraction contains endoplasmic reticulum and Golgi apparatus, where *N*-linked oligosaccharides are constructed. The predominance of high-mannose-type oligosaccharides in the soluble fraction may be the cause of immature oligosaccharides in the process of biosynthesis. In contrast, complex and hybrid types with or without sialic acids were detected in the insoluble fraction, suggesting that membrane proteins carry mature oligosaccharides.

In addition, GCC-LC/MS revealed differences in glycosylation between control cells and aberrant model cells. Biantennary forms bearing extra GlcNAc were obviously increased in cells transfected with the GnT-III gene, indicating that our methodology allows us to explore changes in the glycosyltransferase expression followed by glycan alteration. Although MS is frequently used for the analysis of glycosylation, identification of oligosaccharide isomers by MS alone

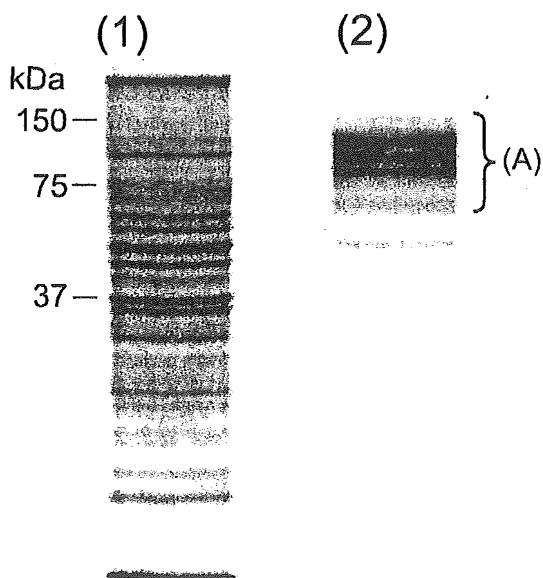

Figure 4. (1) 1-D SDS-PAGE and (2) lectin blot images of the CHO-III insoluble fraction. Proteins were separated on a 12.5% SDS-PAGE gel and stained with SYPRO Orange.

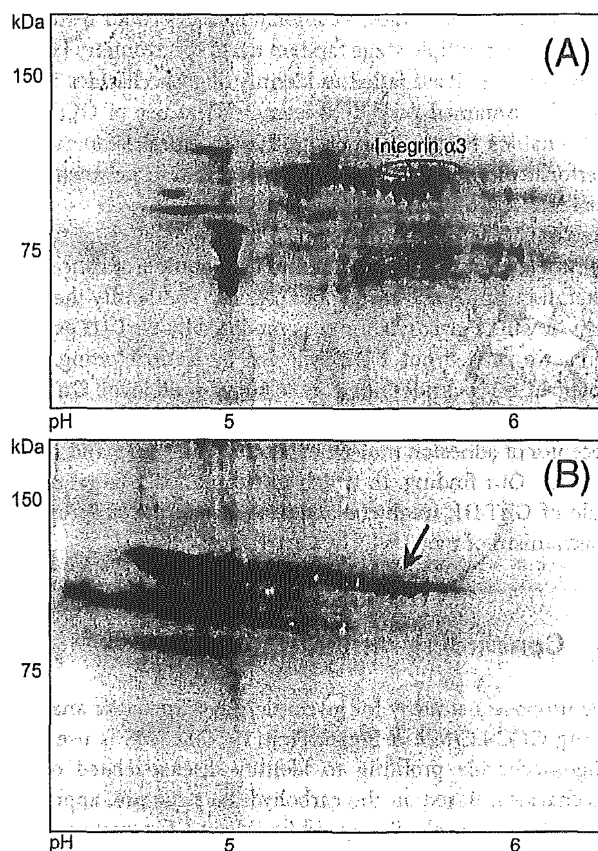

Figure 5. Enlarged partial (A) 2-DE and (B) lectin blot images from band A in Fig. 4.

© 2005 WILEY-VCH Verlag GmbH & Co. KGaA, Weinheim

still remains challenges. Positional isomers could be differentiated by multiple-stage tandem mass spectrometry (MS^n); however, MS^n itself failed to identify oligosaccharides if the sample contained positional isomers. The use of GCC-LC/MS enables us to differentiate the structural isomers and perform differential analysis in glycosylation between normal and aberrant cells.

GnT-III is reported to involve the suppression of tumor cell metastasis and is assumed to be a marker of cancerous alteration in hepatic carcinoma [21, 22]. To identify the protein in which glycosylation was modified by GnT-III expression, we carried out 2-DE followed by lectin blotting, and Integrin α3 was identified as a target protein of GnT-III. Integrin α3, a type I membrane protein, is known to be a receptor of adhesion molecules, such as laminin 5 and 10/11 [23–25]. Our finding, in which integrin α3 is a target molecule of GnT-III, might be a clue to clarify the suppression mechanism of metastasis by GnT-III.

5 Concluding remarks

We propose a strategy for glycomic/glycoproteomic analysis using GCC-LC/MS in Fig. 6. First, GCC-LC/MS is used for oligosaccharide profiling to identify disease-related oligosaccharides. Based on the carbohydrate structure, appropriate lectins or antibodies could be selected for western blotting. Proteins carrying disease-related oligosaccharides could then be identified by 2-D lectin blotting followed by MS/MS analysis. Using several groups, 2-D lectin blotting has been proposed for the characterization of glycoproteins on gel [26, 27]. The use of mass spectrometric oligosaccharide profiling, which can directly characterize glycan structures, is worthwhile to obtain structural information about disease-related carbohydrate and is helpful in the subsequent choice of appropriate lectins and antibodies. Our method is expected to be a powerful tool for glycomic/glycoproteomic analysis.

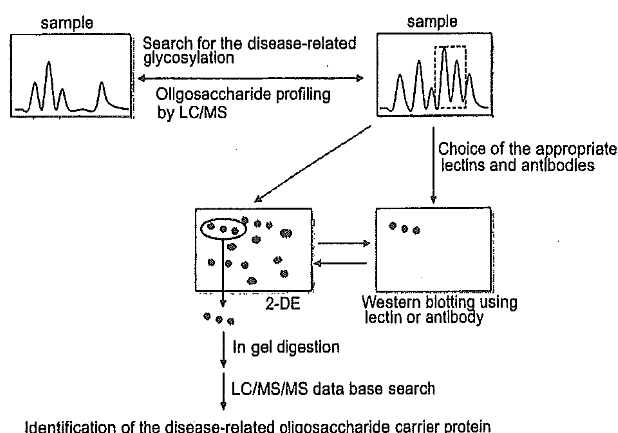

Figure 6. Strategy for glycomics/glycoproteomics using GCC-LC/MS, 2-DE and 2-D Western blotting using lectin or antibody.

6 References

[1] Varki, A., *Glycobiology* 1993, *3*, 97–130.

[2] Isaji, T., Gu, J., Nishiuchi, R., Zhao, Y. *et al., J. Biol. Chem.* 2004, *279*, 19747–19754.

[3] Stanley, P., *Biochim. Biophys. Acta* 2002, *1573*, 363–368.

[4] Schachter, H., *Cell Mol. Life Sci.* 2001, *58*, 1085–1104.

[5] Dennis, J. W., Granovsky, M., Warren, C.E., *Biochim. Biophys. Acta* 1999, *1473*, 21–34.

[6] Delves, P. J., *Autoimmunity* 1998, *27*, 239–253.

[7] Gleeson, P. A., *Biochim. Biophys. Acta* 1994, *1197*, 237–255.

[8] Chui, D., Sellakumar, G., Green, R., Sutton-Smith, M. *et al., Proc. Natl. Acad. Sci. USA* 2001, *98*, 1142–1147.

[9] Itoh, S., Kawasaki, N., Ohta, M., Hyuga, M. *et al., J. Chromatogr. A* 2002, *968*, 89–100.

[10] Kawasaki, N., Haishima, Y., Ohta, M., Itoh, S. *et al., Glycobiology* 2001, *11*, 1043–1049.

[11] Kawasaki, N., Ohta, M., Itoh, S., Hyuga, M. *et al., Biologicals* 2002, *30*, 113–123.

[12] Davies, M., Smith, K. D., Harbin, A. M., Hounsell, E. F., *J. Chromatogr.* 1992, *609*, 125–131.

[13] Narasimhan, S., *J. Biol. Chem.* 1982, *257*, 10235–10242.

[14] Yoshimura, M., Ihara, Y., Matsuzawa, Y., Taniguchi, N., *J. Biol. Chem.* 1996, *271*, 13811–13815.

[15] Taniguchi, N., Miyoshi, E., Ko, J. H., Ikeda, Y., Ihara, Y., *Biochim. Biophys. Acta* 1999, *1455*, 287–300.

[16] Yoshimura, M., Nishikawa, A., Ihara, Y., Taniguchi, S., Taniguchi, N., *Proc. Natl. Acad. Sci. USA.*1995, *92*, 8754–8758.

[17] Bhaumik, M., Harris, T., Sundaram, S., Johnson, L. *et al., Cancer Res.* 1998, *58*, 2881–2887.

[18] Laemmli, U. K., *Nature* 1970, *227*, 680–685.

[19] Stanley, S., Sundaram, S., Tang, J., Shi, S., *Glycobiology* 2005, *15*, 43–53.

[20] Lee, J., Sundaram, S., Shaper, N. L., Raju, S., Stanley, P., *J. Biol .Chem.* 2001, *276*, 13924–13934.

[21] Yamashita, K., Koide, N., Endo, T., Iwaki, Y., Kobata, A., *J. Biol. Chem.* 1989, *264*, 2415–2423.

[22] Yamashita, K., Hitoi, A., Taniguchi, N., Yokosawa, N. *et al., Cancer Res.* 1983, *43*, 5059–5063.

[23] Carter, W. G., Ryan, M. C., Gahr, P. J., *Cell* 1991, *65*, 599–610.

[24] Kikkawa, Y., Umeda, M., Miyazaki, K., *J. Biochem (Tokyo)* 1994, *116*, 862–869.

[25] Kikkawa, Y., Sanzen, N., Sekiguchi, K., *J. Biol. Chem.* 1998, *273*, 15854–15859.

[26] Kim, Y. S., Hwang, S. Y., Oh, S., Shon, H. *et al., Proteomics* 2004, *4*, 3353–3358.

[27] Rahman, M. A., Karsani, S. A., Othman, I., Rahman, P. S. A., Hashim, O. H., *Biochem. Biophys. Res. Commun.* 2002, *295*, 1007–1013.

© 2005 WILEY-VCH Verlag GmbH & Co. KGaA, Weinheim

ELSEVIER

Available online at www.sciencedirect.com

SCIENCE DIRECT®

Journal of Chromatography A, 1067 (2005) 145–152

JOURNAL OF CHROMATOGRAPHY A

www.elsevier.com/locate/chroma

Isotope tag method for quantitative analysis of carbohydrates by liquid chromatography–mass spectrometry

Jin Yuan[1], Noritaka Hashii, Nana Kawasaki*, Satsuki Itoh, Toru Kawanishi, Takao Hayakawa

Division of Biological Chemistry and Biologicals, National Institute of Health Sciences, 1-18-1 Kamiyoga, Setagaya-ku, Tokyo 158-8501, Japan

Available online 15 December 2004

Abstract

We have previously demonstrated that liquid chromatography/mass spectrometry equipped with a graphitized carbon column (GCC-LC/MS) is useful for the structural analysis of carbohydrates in a glycoprotein. Here, we studied the monosaccharide composition analysis and quantitative oligosaccharide profiling by GCC-LC/MS. Monosaccharides were labeled with 2-aminopyridine and then separated and monitored by GCC-LC/MS in the selective ion mode. The use of tetradeuterium-labeled pyridylamino (d_4-PA) monosaccharides as internal standards, which were prepared by the tagging of standard monosaccharides with hexadeuterium-labeled 2-aminopyridine (d_6-AP), afforded a good linearity and reproducibility in ESIMS analysis. This method was successfully applied to the monosaccharide composition analysis of model glycoproteins, fetuin, and erythropoietin. For quantitative oligosaccharide profiling, oligosaccharides released from an analyte and a standard glycoprotein were tagged with d_0- and d_6-AP, respectively, and an equal amount of d_0- and d_4-PA oligosaccharides were coinjected into GCC-LC/MS. In this procedure, the oligosaccharides that existed in either analyte or a standard glycoprotein appeared as single ions, and the oligosaccharides that existed in both analyte and a standard glycoprotein were detected as paired ions. The relative amount of analyte oligosaccharides could be determined on the basis of the analyte/internal standard ion-pair intensity ratio. The quantitative oligosaccharide profiling enabled us to make a quantitative and qualitative comparison of glycosylation between the analyte and standard glycoproteins. The isotope tag method can be applicable for quality control and comparability assessment of glycoprotein products as well as the analysis of glycan alteration in some diseases.
© 2004 Elsevier B.V. All rights reserved.

Keywords: Monosaccharides; Oligosaccharides; Pyridylamination; Isotope tag

1. Introduction

A variety of recombinant glycoproteins and modified glycoproteins are developed as medical agents, and most of them exist in heterogeneous forms because of the various combinations of oligosaccharides. Alteration of glycosylation is known to affect the biological activity, mobilization, and biophysical properties of glycoproteins [1], so assessments of their carbohydrate structure and heterogeneity are essential in many stages of development and quality control of glycoprotein products. Since glycosylation varies in response to changes in the manufacturing condition, monosaccharide composition analysis and/or oligosaccharide profiling are needed for the characterization and as a test for constancy and comparability assessments of glycosylation [2]. Several analytical procedures using HPLC have been reported for oligosaccharide profiling and structural analysis of carbohydrates [3–5]. The oligosaccharide profiling using liquid chromatography/mass spectrometry (LC/MS) is especially known to provide structural information from their chromatographic behavior and molecular mass [6–8]. We have developed mass spectrometric oligosaccharide profiling using a graphitized carbon column (GCC), which can separate

Abbreviations: AP, 2-aminopyridine; d_0, non-deuterium-labeled; d_4, tetradeuterium-labeled; d_6, hexadeuterium-labeled; Fuc, fucose; Gal, galactose; GalN, galactosamine; GalNAc, *N*-acetylgalactosamine; GCC, graphitized carbon column; Glc, glucose; GlcN, glucosamine; GlcNAc, *N*-acetylglucosamine; Man, mannose; PA, pyridylamino; R.S.D., relative standard deviation; SIM, selected ion mode; TFA, trifluoroacetic acid; TIC, total ion chromatogram

* Corresponding author. Tel.: +81 3 3700 1141; fax: +81 3 3707 6950.
E-mail address: nana@nihs.go.jp (N. Kawasaki).

[1] Present address: Chendu Institute of Biological Products, 610063, Chengdu Wai Dong Bao Jiang Qiao, Sichuan Province, China.

0021-9673/$ – see front matter © 2004 Elsevier B.V. All rights reserved.
doi:10.1016/j.chroma.2004.11.070

oligosaccharides based on subtle differences in branch, position, and linkage with volatile solution [9,10]. This method enables us to distinguish the glycosylation among some glycoprotein products produced in different cells [11].

A use of internal standards is known to improve the precision and linearity in quantitative analyses. Isotopic analogs of the analytes are currently the preferred internal standards for quantification by mass spectrometry (MS) procedures. For instance, Gygi et al. [12] demonstrated the approach for the accurate quantification of the proteins within complex mixture using isotope-coded affinity tags (ICATs). The use of the isotope-labeled carbohydrates as internal standards can make it possible to quantify the carbohydrates by LC/MS. Reductive pyridylamination is frequently used for the tagging of carbohydrates in HPLC analysis [13,14]. This derivatization is known to afford higher sensitivity in MS analysis [15], and PA oligosaccharides were reported to be separated by GCC [16]. Here, we study quantitative analysis of carbohydrates using tetradeuterium-labeled pyridylamino (d_4-PA) carbohydrates as internal standards. First, we study the monosaccharide composition analysis by using d_4-PA monosaccharides as internal standards. Next, the isotope tag method is used for the quantitative oligosaccharide profiling using recombinant human chorionic gonadotropin (rhCG) and human chorionic gonadotropin (hCG) as an analyte and standard glycoproteins, respectively.

2. Materials and methods

2.1. Materials

All monosaccharide standards were purchased from Seikagaku-kogyo (Tokyo, Japan). The pyridylamination apparatus (PALSTATION), reagents for the pyridylamination reaction, and PA monosaccharide standards were available from TaKaRa Biomedicals (Otsu, Japan). The hexadeuterium-labeled 2-aminopyridine (d_6-AP) was purchased from Wako (Osaka, Japan). Human chorionic gonadotropin (hCG) and recombinant hCG (rhCG) were bought from Sigma (St. Louis, MO, USA). *N*-glycosidase F was purchased from Roche Diagnostics. All other chemicals and reagents were of analytical grade and were commercially available.

2.2. Pyridylamination of monosaccharides

For the pyridylamination of amino sugars, free amino groups of monosaccharides (GlcN, GalN, 1–1000 pmol) were acetylated by incubation in 50 μl of methanol/pyridine/distilled water (30/15/10, v/v/v) with 2 μl of acetic anhydride for 30 min at room temperature. The mixture was dried using a vacuum centrifuge evaporator without heating. Acetic acid (50 μl), methanol (60 μl), and 10 μl of coupling reagent prepared by mixing 100 mg of AP was added to monosaccharides (Fuc, Gal, Glc, Man, GlcNAc, GalNAc, 1–1000 pmol). The mixture was heated at 90 °C for 20 min by PALSTATION, and the excess reagents were removed by evaporation under a stream of nitrogen gas at 60 °C for 20 min. Then 10 μl of a reducing reagent, prepared just before use by mixing 6 mg of borane–dimethylamine complex and 100 μl of acetic acid, was added, and the mixture was heated at 90 °C for 35 min. The reaction mixture was dried three times under a stream of nitrogen gas at 50 °C for 10 min. The residue was dissolved in water for LC/MS analysis. For the preparation of isotope analogs, the tetradeuterium-labeled PA (d_4-PA) monosaccharide, d_0-AP was just replaced by d_6-AP (Fig. 1).

2.3. Monosaccharide composition analysis of a glycoprotein

A glycoprotein (25 pmol) was placed in a hydrolysis tube fitted with a Teflon-lined screw cap. Fifty microliters of 2 M HCl-2M trifluoroacetic acid (TFA) was added to the sample, which was then heated at 100 °C for 6 h. Simultaneously, a set of monosaccharide standards, 100 pmol of Gal, Man, Glc, Fuc, GlcN, and GalN, was treated identically as the analytes. The solution obtained was freeze-dried. The monosaccharides obtained from the analyte glycoproteins and standard monosaccharides were tagged with non-deuterium-labeled 2-aminopyridine (d_0-AP) and d_6-AP, respectively. Each tagged oligosaccharide mixture was dissolved into purified water, and a mixture of d_0- and d_4-PA monosaccharides was injected into the GCC-LC/MS.

2.4. Preparation of N-linked oligosaccharides

N-linked oligosaccharides were released from hCG as described previously [17]. Briefly, hCG and rhCG (100 μg)

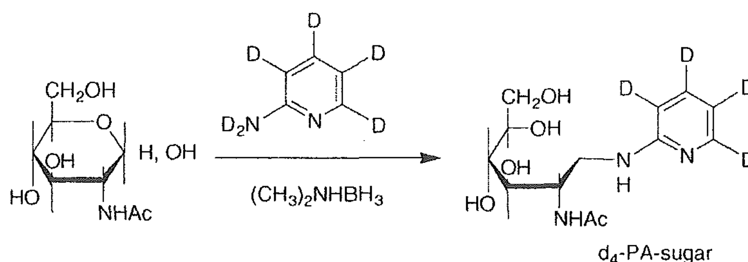

Fig. 1. Synthesis of d_4-PA monosaccharide internal standard.

were dissolved in 360 μl of 0.5 M Tris–HCl buffer (pH 8.6), containing 8 M guanidine hydrochloride and 5 mM ethylenediaminetetra-acetic acid (EDTA). After an addition of 2.6 μl of 2-mercaptethanol, the mixture was allowed to stand at room temperature for 2 h. To this solution, 7.56 mg of monoiodoacetic acid was added, and the resulting mixture was incubated at room temperature for 2 h in the dark. The reaction mixture was applied to a PD-10 column (Amershambioscience, Uppsala, Sweden) to remove the reagents, and the eluate was lyophilized.

Carboxymethylated hCG and rhCG were dissolved in 100 μl of 0.1 M sodium phosphate buffer, pH 7.2, and incubated with 5 units of PNGase F at 37 °C for 2 days. Protein was precipitated with 340 μl of cold ethanol, and the supernatant was dried.

2.5. Pyridylamination of oligosaccharides from hCG

To the lyophilized oligosaccharides released from rhCG we added 10 μl of coupling reagent prepared by mixing 300 mg of d_0-AP, and 100 μl of acetic acid, and the reaction mixture was heated at 90 °C for 60 min. Then, 10 μl of a reducing reagent, prepared just before use by mixing 20 mg of borane–dimethylamine complex and 100 μl of acetic acid, was added, and the mixture was heated at 80 °C for 60 min. The reaction mixture was dried three times under a stream of nitrogen gas at 60 °C for 10 min. The residue was dissolved in water for LC/MS analysis. For the preparation of the tetradeuterium-labeled (d_4)-PA oligosaccharide isotope analogs, d_0-AP was just replaced by d_6-2-aminopyridine.

2.6. LC/MS analysis

LC was carried out using a Magic 2002 HPLC system (Michrom BioResources Inc., Auburn, CA, USA) using a Hypercarb column (0.2 mm × 150 mm, Thermoelectron, San Jose, CA, USA). The flow rate was set at 2–3 μl/min through a splitter system. The mobile phases were 5 mM ammonium acetate (pH 8.5) with 2% of acetonitrile (pump A) and 80% of acetonitrile (pump B). A gradient of 10–35% of B in 60 min was used for the monosaccharide analysis. For oligosaccharide profiling, we used a gradient of 5–20% of B in 20 min, 20–70% of B in 15 min, and 70–95% of B in 5 min. The mass spectrometer used was a TSQ 7000 (Thermoelectron) equipped with a nanoelectrospray ion source (AMR Inc., Tokyo, Japan). The ESI voltage was set to 2000 V (positive ion mode) or 1500 V (negative ion mode), and the capillary temperature was 175 °C.

3. Results

3.1. Monosaccharide composition analysis using the isotope tag method

First, we examined the possibility of the isotope-tag method for the monosaccharide composition analysis of gly-

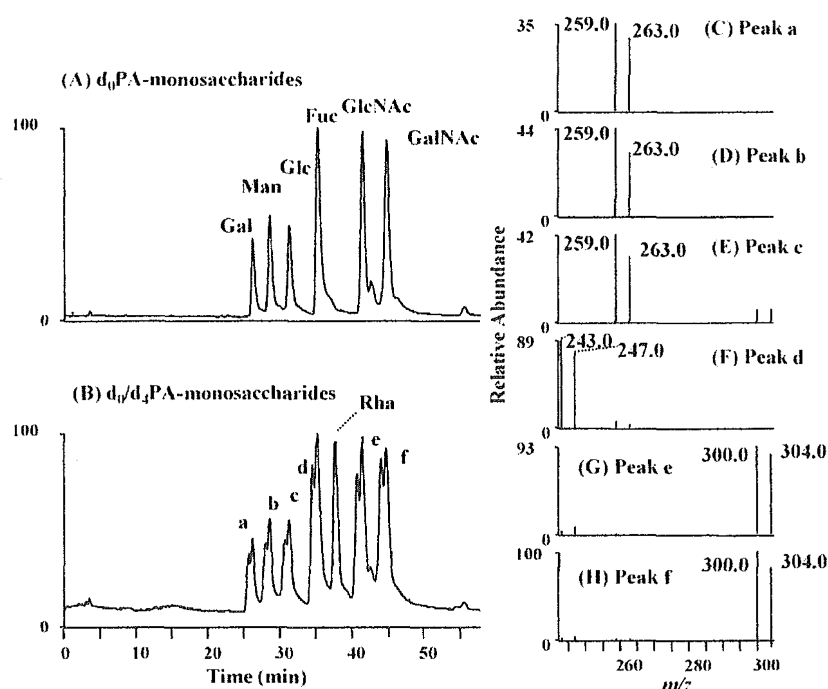

Fig. 2. (A) Extracted ion chromatogram (set *m/z* values, 243, 259, and 300) of d_0-PA monosaccharides (1 pmol Gal, Man, Glc, Fuc, GlcNAc, and GalNAc). (B) Extracted ion chromatogram (set *m/z* values, 243, 247, 259, 263, 300, and 304) of a mixture of d_0- and d_4-PA monosaccharides (1 pmol Gal, Man, Glc, Fuc, Rham, GlcNAc and GalNAc). (C) Mass spectra of peaks a (C), b (D), c (E), d (F), e (G), and f (H).

coproteins. An equal molar of each d_0-PA monosaccharide (Gal, Man, Glc, Fuc, GlcNAc, and GalNAc, 1 pmol each) was analyzed by GCC-LC/MS in the positive ion mode. The ions monitored were *m/z* 259 (for d_0-PA-Gal, d_0-PA-Man, and d_0-PA-Glc), *m/z* 243 (d_0-PA-Fuc), and *m/z* 300 (d_0-PA-GlcNAc and d_0-PA-GalNAc). Fig. 2A shows the mass chromatogram of the d_0-PA monosaccharides. All six d_0-PA monosaccharides were retained and separated by GCC. The detection limit at a signal-to-noise ratio of 3 was 45 fmol.

The d_4-PA monosaccharides were prepared as internal standards by tagging of standard monosaccharides with d_6-AP and combined with d_0-PA monosaccharides. Fig. 2B shows the chromatogram of a mixture of d_0-, d_4-PA monosaccharides and PA-labeled Rhamnose, which is frequently used as an internal standard in the monosaccharide composition analysis. Paired ions with a difference of *m/z* 4 were detected in the mass spectra of peaks a–f (Fig. 2C–H). When 0.5 pmol d_0-PA monosaccharides were determined in the presence of d_4-PA monosaccharides or Rhamnose by GCC-LC/MS, the relative standard deviation ($n = 5$) was 1.8–4.8% or 5.6–8.3%, respectively.

To assess the linearity and reproducibility of the whole procedure, including reacetylation, pyridylamination, the removal of excess derivatization reagents, and GCC-LC/MS, we tagged different amounts of monosaccharides (Gal, Man, Glc, Fuc, GlcN, and GalN, 1–1000 pmol) with d_0-AP, and d_4-PA monosaccharides (4 or 20 pmol) were added to the d_0-PA monosaccharides (1–10 pmol or 10–1000 pmol, respectively). The whole process of the isotope tag method was found to be linear for all six monosaccharides over the tested range of 1–1000 pmol (Fig. 3). The accuracy of this method was approximately 80–100% (Fig. 3), and the relative standard deviations (%R.S.D.) were less than 7.2% for all monosaccharides (based on the peak area ratio of monosaccharides from five samples).

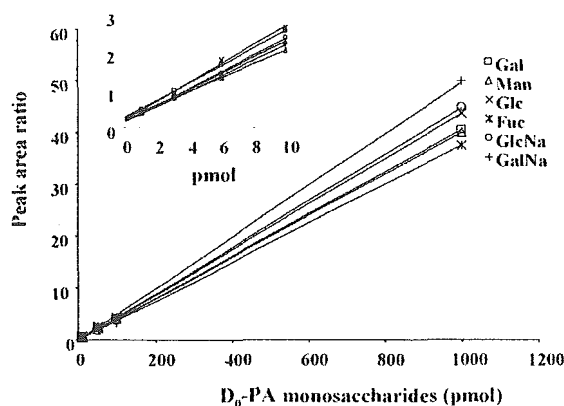

Fig. 3. Linearity on the isotope-tag method for monosaccharide quantification. For the internal standards, 1000 pmol monosaccharides were derivatized to d_4-PA monosaccharides. Different amounts of monosaccharides were derivatized to d_0-PA monosaccharides and co-injected with 4 pmol (A) or 20 pmol (B) internal standards into GCC-LC/MS.

We used this method for the monosaccharide composition analysis of fetuin and erythropoietin. Accuracy in the monosaccharide composition analysis of a glycoprotein relies on the condition of hydrolysis. Fan et al. [18] studied the hydrolysis of N-linked oligosaccharides and recommended 4 h with 2 M TFA at 100 °C for neutral sugars, and 6 h with 4 M HCl at 100 °C for amino sugars. While these hydrolysis conditions result in the complete release of neutral and amino sugars with no degradation, it takes two hydrolyses for a single sample. To quantify both neutral and amino sugars in glycoproteins in the same run, fetuin and erythropoietin (25 pmol) were heated in 2 M HCl-2M TFA at 100 °C for 6 h [19], and a set of monosaccharide standards, 100 pmol of Gal, Man, Glc, Fuc, GlcN, and GalN, was treated identically as the analyte glycoproteins. After hydrolysis, the analyte and standard monosaccharides were tagged with d_0- and d_6-AP, respectively. Fig. 4A and E show the mass chromatogram of monosaccharides prepared from fetuin and erythropoietin in the presence of d_4-PA monosaccharides, respectively.

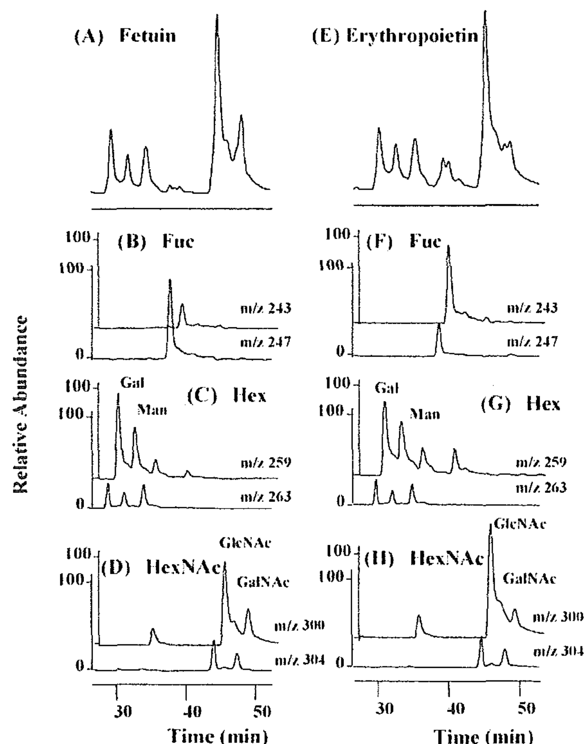

Fig. 4. Monosaccharide composition analysis of glycoproteins. Extracted ion chromatograms of d_0-PA monosaccharides from fetuin and d_4-PA standard monosaccharides (set *m/z* values, 243, 247, 259, 263, 300, and 304) (A), d_0-PA Fuc from fetuin and d_4-PA standard Fuc (set *m/z* values, 243 and 247) (B), d_0-PA Hex from fetuin and d_4-PA standard Hex (set *m/z* values, 259 and 263) (C), and d_0-PA HexNAc from fetuin and d_4-PA standard HexNAc and (set *m/z* values, 300 and 304) (D). Extracted ion chromatograms of d_0-PA monosaccharides from erythropoietin and d_4-PA standard monosaccharides and (set *m/z* values, 243, 247, 259, 263, 300, and 304) (E), d_0-PA Fuc from erythropoietin and d_4-PA standard Fuc (set *m/z* values, 243 and 247) (F), d_0-PA Hex from erythropoietin and d_4-PA standard Hex (set *m/z* values, 259 and 263) (G), and d_0-PA HexNAc from erythropoietin and d_4-PA standard HexNAc (set *m/z* values, 300 and 304) (H).